

CO₂ Laser Induced Decomposition of Freon 113

Jeffrey J.^{Joseph} Rusik UC 1979
///

Submitted in partial fulfillment
of the requirements for
Honors in the Department of Chemistry

Union College
March 24, 1979

UN 82
R 955c
1979

ABSTRACT

RUSIK, JEFFREY CO₂ Laser Induced Decomposition of
Freon 113. Department of Chemistry March, 1979.

Gaseous freon 113, or CCl₂FCClF₂, was irradiated with a continuous wave carbon dioxide infrared laser. The rate of formation of CF₂CClF, a decomposition product, was monitored using an infrared spectrometer. The initial rates of product formation were related to irradiation wavelength and power, and the laser induced reaction was related to pyrolysis decomposition. A computer program which calculates the temperatures in a laser beam is modified and applied to the irradiations performed. It is determined that bi- or triphotonic absorption is occurring and that the laser induced reactions are photocatalyzed. A reaction model is discussed which combines thermal excitation, multiphotonic absorption, and collisional vibrational activation.

ABSTRACT

RUSIK, JEFFREY CO₂ Laser Induced Decomposition of
Freon 113. Department of Chemistry March, 1979.

Gaseous freon 113, or CCl₂FCClF₂, was irradiated with a continuous wave carbon dioxide infrared laser. The rate of formation of CF₂CClF, a decomposition product, was monitored using an infrared spectrometer. The initial rates of product formation were related to irradiation wavelength and power, and the laser induced reaction was related to pyrolysis decomposition. A computer program which calculates the temperatures in a laser beam is modified and applied to the irradiations performed. It is determined that bi- or triphoton absorption is occurring and that the laser induced reactions are photocatalyzed. A reaction model is discussed which combines thermal excitation, multiphotonic absorption, and collisional vibrational activation.

Acknowledgements

I would like to thank Richard Herrick for his invaluable help in familiarizing me with the experimental facets of this project and getting me started on the right foot.

I would like to thank Dr. Thomas Galantowicz for the use of the infrared laser and for his help in its use and maintenance. I also thank Dr. David Peak and his students for the development of the computer program used in this project. I am particularly grateful to John Samuelian and David Marker for their essential help and moral support. I owe special thanks to Dr. Les Hull whose helpful insight and prodding as my research advisor helped to make this project one of the finest learning experiences I have ever known.

Table of Contents

| | |
|------------------------------------|-----|
| Abstract | i |
| Acknowledgements | ii |
| Table of Contents | iii |
| Introduction | 1 |
| Experimental | 14 |
| Results | 20 |
| Discussion | 54 |
| Suggestions for Further Work | 65 |
| Appendix | 67 |
| References | 72 |

Introduction

The development of the laser has had a profound impact on many of the sciences in the past decade. Although laser related work has steadily expanded into such fields as Engineering, Meteorology, and Art, one of the most intriguing applications to which lasers have been put is the controlled stimulation of chemical reactions. Chemists are now exploiting the unique properties of lasers to learn more about the basic processes occurring in chemical reactions and how to modify and control them.¹

Laser radiation is polarized, coherent (in phase), intense, and extremely monochromatic. Clearly laser light interacting with matter may involve various chemical effects, such as photochemical reaction, thermal agitation, equilibrium and non-equilibrium plasma chemistry, chemical reactions in a shock wave, processes caused by an intense ultrasonic field and radioactive radiation.² Of immediate technological importance is laser thermal chemistry, which is now being used for the surface reactions involved in circuit microminiaturization.

A field which is currently of great research interest is laser photochemistry. The highly monochromatic and dense energy flux of laser light can provide, at least in principle, selective excitation of an electronic or vibrational state, selective ionization of a particular atom, or selective

breakage of a chemical bond in the non-thermal stimulation of chemical reactions.² This selectivity is a result of the specific energy of the laser radiation being in resonance with a particular vibrational or electronic transition energy. The extremely monochromatic nature of the laser radiation is selective enough to distinguish between even atomic isotopes.

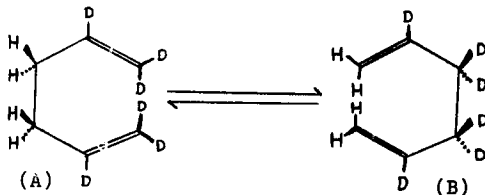
An infrared laser assisted photodissociation can be theoretically discussed by considering the non-thermal equilibrium conditions of laser light absorption and the vibrational weakening of a particular bond. A chemical reaction consists of breaking some chemical bonds and creating others. These bonds are responsible for part of the infrared vibrational spectrum of a molecule. There are specific quantum mechanical (eigen) vibrational frequencies for different bonds. The vibrations in a molecule can be excited by interaction with electromagnetic laser radiation when the frequency of the radiation is in resonance with the eigenfrequency of the bond's vibration. The monochromaticity of laser radiation makes it possible to excite selected vibrational modes, while thermal excitation excites all modes.³

The vibrational absorption of a photon of laser light will greatly increase the temperature of one vibrational mode of a molecule, while temporarily leaving the other modes unaffected. This results in a non-Boltzmann distribution of molecules populating the various vibrational states.

This is defined as non-thermal equilibrium. If the excited bond can dissociate before thermally equilibrating (among the other vibrational, rotational, and translational degrees of freedom) the reaction is photochemically laser controlled.

Photochemistry was previously considered to occur only in an electronically excited state.⁴ Glatt and Yogev, however, stimulated the following Cope reaction with an infrared laser giving a decidedly photochemical reaction without electronic excitation.

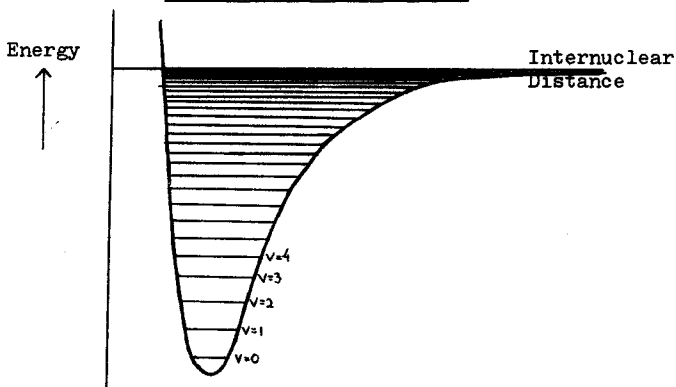
Figure 1: Glatt and Yogev Cope Reaction⁵



It was found that (B) preferentially absorbed radiation and photoisomerized, but at the lasing frequency used (A) did not react. This reaction proceeded by isotopically selective vibrational stimulation in the electronic ground state.

Superimposing the bond length potential well diagram and the vibrational energy states of that bond shows that a bond can be broken by absorbing the appropriate amounts of energy necessary to climb the vibrational energy ladder.

Figure 2: Potential Well -⁶
Vibrational State Diagram



If an infrared photon from a laser hits a molecule with a vibrational transition in resonance with the photon, the molecule will absorb the photon and go into an excited vibrational state. If the molecule absorbs enough of these infrared quanta so that the total energy absorbed equals or exceeds the dissociation energy, the molecule will instantaneously dissociate. In general, the energy of an infrared photon (about 3 kcal/mole) is small compared to bond dissociation energies (generally 30-100 kcal/mole) so multiphoton absorption appears necessary for reaction to occur. Due to the anharmonicity of the potential well, which makes the energy differences between vibrational levels smaller for the higher energy states, the laser radiation can only be in resonance with one or two vibra-

tional excitations.

It is not necessary to absorb enough quanta to exceed the activation energy of a reaction (presumably the bond dissociation energy) to affect a reaction rate, however. If a reaction is considered in which the dissociation of one bond constitutes the energy of activation, the vibrational excitation of that bond will lower the activation energy by the amount of energy absorbed. This excitation will also greatly increase the vibrational temperature of that mode. These changes can be related to the rate of reaction by the Arrhenius equation:

$$k = A \exp(-E^*/RT) \quad (\text{Equation 1})^6$$

where k is the rate constant, A is a constant, E^* is the activation energy for an unexcited molecule, R is the universal gas constant, and T is the absolute temperature.

There have been two different suggestions as to how the laser light absorption affects the Arrhenius rate constant. One involves the substitution of the vibrational temperature (T_{vib}) for the reaction temperature (T).

$$k = A \exp(-E^*/RT_{\text{vib}}) \quad (\text{Equation 2})^2$$

This substitution supposedly presents the main idea of stimulating chemical reactions by infrared laser light.² The problem with this theory is that it neglects the laser's effect on the activation energy.

The equation more commonly cited in literature involves only the effect of the laser on the activation energy.

$$k = A \exp[(nh\nu - E^*)/RT] \quad (\text{Equation 3})^7$$

where n is the number of photons absorbed per molecule and $h\nu$ is the energy of one photon. The problem with this equation is that it is unclear what to use for the temperature value for the non-Boltzmann energy state distribution involved in a photochemical reaction of this nature. Use of the temperature before lasing, i.e. the temperature of the unaffected modes, will yield a low rate constant, and use of the vibrational temperature of the excited mode gives a value which is too high.⁷ It is clear, however, that both effects will increase the rate of reaction.

There are a great number of interactions and transformations possible between the instant of laser photon absorption and reaction initiation, such as vibrational-vibrational, vibrational-rotational, and vibrational-translational relaxations. These processes occur mainly through collisions.² The incidence of reaction under these circumstances therefore depends on whether or not the reaction rate increase due to absorption is sufficient to exceed the rate of the relaxation processes.⁷ This suggests that the maximum photochemical control possible with a laser would be found in a collisionless system. This condition can be approached by using very low pressures. High laser power will also promote photochemical control by speeding the energy collection in the mode of interest so that it overcomes the relaxational energy removal from that mode.³

Basov, Oraevsky, and Pankratov have shown that the energy absorption per molecule and the amount of photochemical control are also made more efficient by increasing the laser radiation pulse length and tuning the laser to a single vibration state transition (The absorption of several small resonant quanta is more efficient than one large quantum for a particular vibrational excitation.)^{3,7}

Higher pressures and lower powers have been shown to result in reactions of an increasingly thermal nature (i.e. less dependent on which mode is excited.) Addition and laser irradiation of relatively inert gases also gives thermalization. The addition of such gases as SF₆ has been used by Freeman and Travis to determine whether certain laser reactions were thermal or photochemical.⁸

Other methods of determining the nature of laser induced reactions include gas chromatography, mass spectrometry, and infrared spectrometry product analysis. A particularly useful means of following a laser reaction is isotope product analysis. A mass spectrometer can be used to determine if the reaction is atomic isotope selective (i.e. one isotope bond is preferentially excited.) A chemical reaction of a thermal nature should have no isotopic selectivity.

Since 1970 many facets of laser chemistry have been the subject of research. Kim, Namba, and Taki have studied the decomposition of organic gases by laser heating. The

irradiation of a solid target with a high power pulsed laser allowed virtually instantaneous heating of the target surface to its boiling point. Slow heating techniques cause decomposition to occur during the heating before the desired temperature is reached. An organic gas in contact with the target surface therefore yielded decomposition products much different than those obtained in conventional heating reactions.⁹

Quel and DeHemptinne studied the laser reactions of ethylene at relatively low laser power and high pressure. They determined the influence of the beam intensity and the addition of noble gases. A theoretical expression for the reaction temperature as a function of noble gas concentrations was derived, and the unimolecular laser stimulated reactions were shown to be thermal in nature.¹⁰

Laser induced fluorescence has been the study of many research teams. Richardson and Ismar studied the carbon-dioxide laser induced sparks and fluorescence in molecular gases such as NH_3 , BF_3 , CF_4 , SiF_4 , CCl_2F_2 , and hydrocarbons.¹¹ In an experiment done by Karney, Ronn, Weitz, and Flynn, the vibrational-vibrational energy transfer rate in infrared laser excited CH_3F was calculated. The fluorescence rise-time of one vibrational mode was measured while exciting another mode.¹² Grabiner and Flynn later did a similar study on CH_3Cl . Fluorescence decay was also measured to find the vibrational-rotational/translational relaxation rate.¹³

These transfer rates and their dependence upon pressure are extremely useful in theoretical calculations involved with laser photochemistry. M. Berry used this fluorescence technique to determine the relative vibrational state populations of the products of a laser induced unimolecular photoelimination. This data was used to help formulate an in-depth photochemical reaction mechanism.¹⁴

Lyman and Rockwood performed isotopically selective laser reactions on boron, carbon, and silicon isotopes.¹⁵ This isotopic enrichment has also been found for other atoms including sulfur and hydrogen. (See page 3)

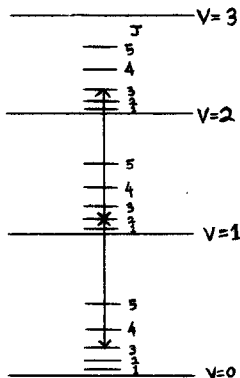
J. K. Thomas has used a visible light laser for monophotonic and biphotonic excitation, and photoionization. He used these forms of excitation in a study of the photolysis of some aromatic compounds such as benzene, naphthalene, and anthracene.¹⁶

V. S. Letokhov has made some speculations on possible uses for the laser in the future. These include ultra-selective bond breaking (molecular surgery), ultrasensitive photoionization, use of the laser to determine the sequence of the DNA nucleotides and perhaps even creating images of molecules with atomic resolution.¹⁷

Several research teams have reported that the irradiation frequency which produces the maximum reaction is of lower energy than the reactant's infrared spectrum absorption maximum. This implies that the laser is not in reso-

nance with the first vibrational transition of the bond being excited. There have been several explanations of this phenomenon. Ambartzumian and Letokhov attributed this to triple photon absorption with the laser tuned to a frequency in the middle of the three resonant frequencies of the first three vibrational energy levels. Resonance is achieved for all three transitions by compensating for the anharmonicity frequency shift with rotational energy.¹⁸ This model was quantum mechanically justified by Oraevsky and Pankratov.¹⁹

Figure 3: Anharmonic Compensation¹⁹
With Rotational Energy



Earl and Ronn noted that the laser induced reaction of fluoromethane and chlorine is essentially independent of irradiation frequency to $\pm 50 \text{ cm}^{-1}$ of the absorption maximum. The sparse vibrational-rotational state density of CH_3F is

inconsistent with the rotational anharmonicity compensation model. Fluoromethane has a large permanent electric dipole moment, so this off-resonance reaction might be explained by first order Stark effect energy shifts (the change of energy levels in a strong electric field.)²⁰

Low power irradiations of boron hydrides by Riley, Opp, and Shatas displayed "red shifting" relative to the room temperature absorption maximum also. This was interpreted as laser heating causing thermal excitation into higher vibrational states, followed by resonance absorption for these states which should be a lower energy transition.²¹

Much work has been done recently by Richard Herrick in the Union College laser laboratory in developing a model for laser induced reactions which combines the thermal and photochemical models.²² In his work with freon 113 it was found that the maximum reaction rate occurred at a lasing frequency lower than the maximum absorption frequency of the bond being excited. In many cases no reaction was detected even though the laser power absorbed was higher than in reaction inducing irradiations at different wavelengths. This is inconsistent with the thermal reaction model.

It was calculated that about 10^9 collisions per second per molecule were occurring at the pressures used. The reaction was run at laser powers far too low to induce the multiphoton absorption necessary to dissociate the molecule. The collisionless photochemical model is therefore not ap-

plicable.

The absorption of four photons would put the molecule into an energy state called the quasi-continuum where quanta of almost any energy can be absorbed due to the closeness of the vibrational and rotational energy states.²³ It was decided that the additional energy necessary for reaction could be obtained from collisions with other excited molecules, but the laser power was far too low for an absorption of four photons. On this basis the photochemical model with collisional assistance was dropped.

A theoretical model was developed in which thermal excitation was followed by the absorption of one or two photons to put the molecule into the quasi-continuum. Collisions with other excited molecules could then provide the extra energy necessary for dissociation. This model was justified by stating that the laser power was high enough for a one or two photon absorption, and the fact that the maximum reaction rate occurred when the laser was in resonance with a vibrational transition energy lower than the $v=0$ to $v=1$ transition.

This research project is a continuation of Richard Herrick's work. It concerns reaction rate and product analysis studies as a function of such variables as lasing frequency, experimental conditions, and absorbed power. The laser induced reactions will be related to hot tube pyrolyses, and photochemical control will be measured. The validity

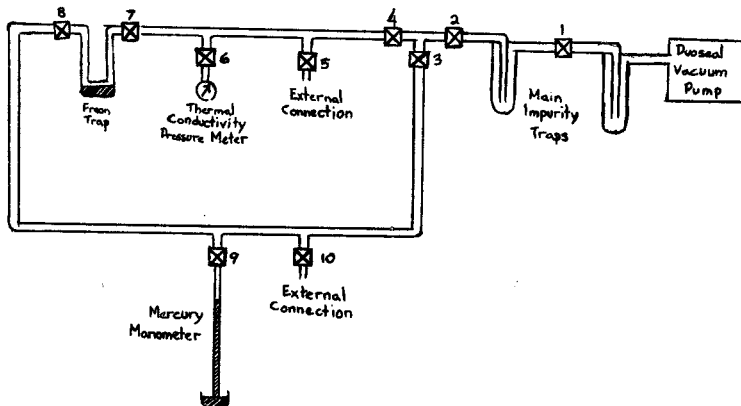
of the thermally enhanced photochemical reaction model will be tested and related to other work done in this field.

Experimental

Sample Preparation

Freon 113 (1,1,2 trichlorotrifluoroethane or $\text{CCl}_2\text{FCClF}_2$) was kept in liquid form in a trap on a glass vacuum line attached to a Duoseal vacuum pump.

Figure 4: Sample Preparation Vacuum Line



The main impurity traps were immersed in liquid nitrogen to protect the pump from undesirable impurities, and then valves 1, 2, 3, 4, 6, and 9 were opened to evacuate the line. The thermal conductivity pressure meter was used to monitor the evacuation. The dissolved gases were removed from the freon by immersing its trap in liquid nitrogen, letting the freon freeze, and opening valve 7 or 8 to let the vol-

atile gases be pumped off. The valve was then closed and the freon allowed to thaw. This degassing was done at least twice before every experimental use.

Two reaction cells were used for this project; an irradiation cell and a pyrolysis cell.

Figure 5: Irradiation Cell

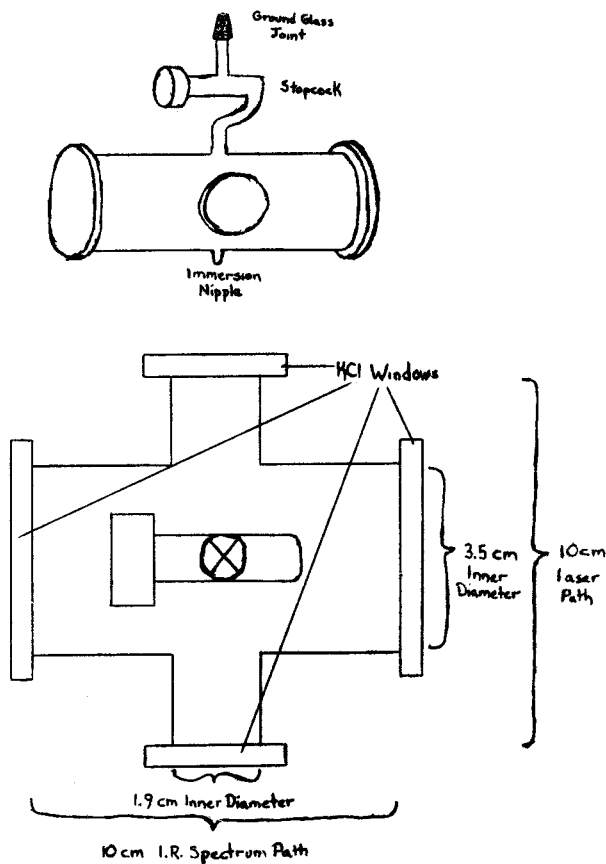
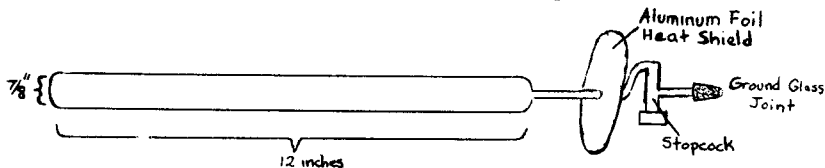


Figure 6: Pyrolysis Cell

The irradiation cell is fitted with potassium chloride windows as shown in figure 5. The windows were glued on using Dow-Corning Silicone Adhesive and Sealer. Periodically these windows were removed for polishing by soaking the glue in toluene. Whenever possible this cell was kept in a dessicator.

Either or both of these cells could be attached to the vacuum line by the external connections. After evacuating the cells, valve 2 was closed and valve 7 or 8 opened until $20.0 \pm .3$ torr of freon was detected by the manometer. The cell stopcocks and external connection valves were then closed and the cells removed.

Cell Window Power Absorption

A potassium chloride cell window was suspended in front of the laser. The power of the laser beam was measured before the window, directly after it, and 10 cm after it. The laser power was varied from 1.7 to 25.8 watts by adjusting the laser current.

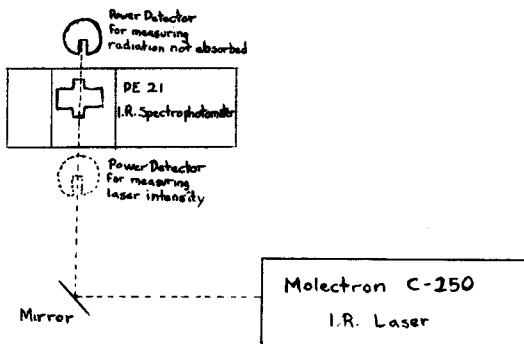
Laser Irradiation

A continuous wave Molelectron Model C-250 Infrared Carbon-Dioxide Gas Laser was used for the irradiations. The laser beam was directed through the small windows of the irradiation cell by a silver coated mirror. The cell was placed on a Perkin Elmer Model 21 Infrared Spectrophotometer so that infrared spectra could be taken during and at right angles to the laser irradiation. A small helium-neon laser was used to align the mirror before irradiation. Bricks were used to block the laser beam when it was not wanted.

Laser beam intensities were measured with a power detector and a Coherent Radiation power meter. Before irradiation, the laser power was measured and checked for constancy. The power out of the back of the cell was monitored continuously during irradiation. Laser beam alignment with the irradiation cell was checked with burn spots on wood and paper.

Infrared spectra in the range $2500-600\text{ cm}^{-1}$ ($4-15\ \mu$) were taken before and after irradiation. During irradiation spectra were taken periodically from $1400-1300\text{ cm}^{-1}$ ($7-8\ \mu$) to monitor the growth of the reaction product peak at 1330 cm^{-1} .

Figure 7: Irradiation Setup



Pyrolysis

The pyrolysis cell containing 20 torr of freon was heated in a Heavy Duty Electrical Company Multiple Unit Tube Heater plugged into a Superior Electric Company Powerstat. (The powerstat and tube heater settings were thermally calibrated using a chromel constantan thermocouple;) Various temperatures and pyrolysis times were used. During the pyrolysis an initial infrared spectrum was taken on freon in the irradiation cell. The irradiation cell was then evacuated, and after pyrolysis the pyrolysis cell was also connected to the vacuum line. Valve 2 was closed and the pyrolysis cell stopcock opened. The immersion nipple of the irradiation cell was then placed in liquid nitrogen to transfer the pyrolysis products to the irradiation cell quantitatively. After this the irradiation cell was closed

off and allowed to warm up in a dessicator (to minimize condensation on the salt windows.) A final infrared spectrum was then taken on the contents of this cell.

Results

Cell Window Power Absorption

The laser was set to 9.6948μ for this determination because this wavelength is roughly in the middle of the irradiation wavelengths used. The following power measurements were obtained.

Table 1: KCl Cell Window Power Absorption

| <u>Power in (w)</u> | <u>Power out (w)</u> | <u>Power 10 cm back (w)</u> |
|---------------------|----------------------|-----------------------------|
| 1.7 | 1.5±.1 | 1.5±.1 |
| 3.0 | 2.7±.1 | 2.6±.1 |
| 3.8 | 3.3±.1 | 3.3±.1 |
| 4.4 | 3.9±.1 | 3.8±.1 |
| 5.0 | 4.4±.1 | 4.4±.1 |
| 6.1 | 5.4±.1 | 5.3±.2 |
| 8.0 | 7.0±.2 | 7.0±.2 |
| 10.5 | 9.4±.2 | 9.3±.2 |
| 13.1 | 11.7±.3 | 11.6±.3 |
| 17.3 | 15.4±.3 | 15.2±.3 |
| 20.4 | 18.2±.4 | 18.0±.4 |
| 23.8 | 21.2±.4 | 20.9±.4 |
| 25.8 | 22.7±.4 | 22.5±.5 |

The uncertainties were determined by moving the window so that the beam went through different parts of it, and the resultant power changes due to window surface aberrations

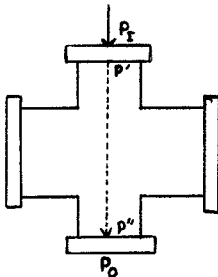
were then recorded as error margins. Window angles of up to 50° off perpendicular to the laser beam had virtually no effect on the power values. Figures 9 and 10 give the following equations:

$$\text{Power out} = (.887)\text{Power in} \quad (\text{Equation 4})$$

$$\text{Power 10 cm back} = (.878)\text{Power in} \quad (\text{Equation 5})$$

These equations express the laser power lost due to absorption, refraction, and reflection while passing through a potassium chloride cell window. The absorption of laser power as it passes through the irradiation cell can now be considered.

Figure 8: Laser Power Absorption
In the Irradiation Cell



P_I = Laser power incident upon the cell

P_O = Laser power leaving the cell (10 cm back)

P' = Laser power entering the sample

P'' = Laser power leaving the sample

To get the laser power absorbed by the sample $P_A = P' - P''$,

P_I and P_O must be measured and applied to equations 4 and 5.

$$P' = (.887)P_I \quad (\text{Equation 6})$$

$$P'' = P_O / (.878) \quad (\text{Equation 7})$$

$$P_A = (.887)P_I - (1.139)P_O \quad (\text{Equation 8})$$

Laser Wavelength Dependent Reaction Rate Study

The growth of the infrared spectrum 1330 cm^{-1} product peak as a function of time was monitored for several irradiation wavelengths. Absorbance versus time graphs were then extrapolated to the origin and initial rate slopes calculated. A typical infrared spectrum (#72) for this part of the project is included as figure 11.

Table 2: Laser Wavelength Reaction
Rate Study

| <u>Laser Wavelength (μ)</u> | <u>Spectrum Number</u> | <u>P_I (w)</u> | <u>P_O (w)</u> | <u>P_A (w)</u> | <u>time (min)</u> | <u>Absorbance</u> |
|--|------------------------|--------------------------|--------------------------|--------------------------|-------------------|-------------------|
| 9.7533 | 72 | 15.0 | 2.1 | 10.9 | 1 | .013 |
| | | | | | 4 | .051 |
| | | | | | 9 | .109 |
| | | | | | 14 | .133 |
| | | | | | 17 | .154 |
| | | | | | 22 | .179 |
| | | | | | 26 | .182 |
| 30 | .183 | | | | | |
| 9.7335 | 62 | 19.3 | 2.9 | 13.8 | 3 | .026 |
| | | | | | 5 | .047 |
| | | | | | 10 | .110 |
| | | | | | 15 | .124 |
| | | | | | 20 | .123 |
| | | | | | 25 | .164 |
| 9.7335 | 69 | 17.3 | 2.3 | 12.7 | 5 | .040 |
| | | | | | 15 | .059 |
| | | | | | 20 | .076 |
| | | | | | 25 | .082 |

Table 2 (continued)

| <u>Laser Wavelength (μ)</u> | <u>Spectrum Number</u> | <u>P_I (w)</u> | <u>P_O (w)</u> | <u>P_A (w)</u> | <u>time (min)</u> | <u>Absorbance</u> |
|--|------------------------|--------------------------|--------------------------|--------------------------|-------------------|-------------------|
| 9.7140 | 52 | 17.3 | 2.5 | 12.5 | 1 | .019 |
| | | | | | 2 | .036 |
| | | | | | 3 | .048 |
| | | | | | 4 | .054 |
| | | | | | 5 | .060 |
| | | | | | 6 | .061 |
| | | | | | 7 | .062 |
| 9.7140 | 68 | 17.0 | 2.3 | 12.5 | 5 | .060 |
| | | | | | 10 | .078 |
| | | | | | 15 | .089 |
| 9.6948 | 67 | 17.2 | 2.2 | 12.8 | 5 | .059 |
| | | | | | 7 | .073 |
| | | | | | 10 | .083 |
| 9.6760 | 71 | 17.4 | 3.0 | 12.0 | 1 | .010 |
| | | | | | 4 | .037 |
| | | | | | 6 | .058 |
| | | | | | 14 | .133 |
| 9.6574 | 70 | 17.3 | 3.3 | 11.6 | 8 | .020 |
| | | | | | 13 | .027 |
| | | | | | 20 | .030 |
| 9.6036 | 61 | 19.2 | 3.5 | 13.0 | 10 | 0.0 |

This data is graphed in Figures 12-19, giving the following initial reaction rates:

Table 3: Initial Reaction Rates at
Different Laser Wavelengths

| <u>Laser Wavelength (μ)</u> | <u>Spectrum Number</u> | <u>P_A (w)</u> | <u>Initial Reaction Rate (min⁻¹)</u> |
|--|------------------------|--------------------------|---|
| 9.7533 | 72 | 10.9 | .013*.007 |
| 9.7335 | 62 | 13.8 | .012*.002 |
| 9.7335 | 69 | 12.7 | .011*.004 |
| 9.7140 | 52 | 12.5 | .022*.002 |

Table 3 (continued)

| <u>Laser Wavelength (μ)</u> | <u>Spectrum Number</u> | <u>P_A (w)</u> | <u>Initial Reaction Rates (min⁻¹)</u> |
|--|------------------------|--------------------------|--|
| 9.7140 | 68 | 12.5 | .024±.003 |
| 9.6948 | 67 | 12.8 | .018±.003 |
| 9.6760 | 71 | 12.0 | .0106±.0006 |
| 9.6574 | 70 | 11.6 | .0033±.0003 |
| 9.6036 | 61 | 13.0 | No detectable reaction |

A graph of these reaction rates is superimposed on the freon 113 infrared absorption spectrum in figure 28.

Laser Power Reaction Rate Study

Infrared spectra were taken during laser irradiations and again the growth of the 1330 cm⁻¹ reaction product peak was monitored. Absorbance versus time was plotted and the initial product formation rates were determined. The laser was set to a wavelength of 9.7140 μ because this corresponds with the maximum rate of reaction. Several laser power levels were used to obtain the following data:

Table 4: Laser Power Reaction Rate Study

| <u>P_I (w)</u> | <u>P_O (w)</u> | <u>P_A (w)</u> | <u>Spectrum Number</u> | <u>time (min⁻¹)</u> | <u>Absorbance</u> |
|--------------------------|--------------------------|--------------------------|------------------------|--------------------------------|-------------------|
| 6.0 | .9 | 4.3 | 52 | 15 | 0.0 |
| 8.7 | 1.1 | 6.4 | 52 | 15 | 0.0 |
| 9.7 | 1.2 | 7.3 | 74 | 20 | .015 |
| | | | | 30 | .016 |
| | | | | 40 | .019 |
| | | | | 50 | .030 |

Table 4 (continued)

| P_I (w) | P_O (w) | P_A (w) | Spectrum Number | time (min^{-1}) | Absorbance |
|-----------|-----------|-----------|-----------------|----------------------------|------------|
| 12.0 | 1.4 | 9.0 | 52 | 10 | 0.0 |
| 15.1 | 2.8 | 10.2 | 85 | 5 | .067 |
| | | | | 8 | .075 |
| | | | | 12 | .095 |
| | | | | 16 | .113 |
| | | | | 25 | .117 |
| | | | | 30 | .122 |
| 17.3 | 2.5 | 12.5 | 52 | 40 | .131 |
| | | | | 1 | .019 |
| | | | | 2 | .036 |
| | | | | 3 | .048 |
| | | | | 4 | .054 |
| | | | | 5 | .060 |
| | | | | 6 | .078 |
| 7 | .089 | | | | |
| 19.5 | 3.8 | 13.0 | 86 | 5 | .157 |
| | | | | 8 | .166 |
| | | | | 10 | .182 |
| 22.0 | 3.1 | 16.0 | 78 | 2 | .116 |
| | | | | 3 | .174 |
| | | | | 4 | .204 |
| | | | | 5 | .234 |
| | | | | 8 | .271 |
| | | | | 8 | .281 |
| 25.5 | 4.5 | 17.5 | 73 | 2 | .088 |
| | | | | 3 | .129 |
| | | | | 4 | .149 |
| | | | | 5 | .171 |
| | | | | 8 | .209 |
| | | | | 10.5 | .230 |

This data is graphed in figures 15 and 20-24, giving the following initial reaction rates:

Table 5: Initial Reaction Rates at
Different Laser Powers

| <u>P_A (w)</u> | <u>ln(P_A)</u> | <u>Spectrum Number</u> | <u>Initial Reaction Rate (min⁻¹)</u> | <u>-ln(Rate)</u> |
|--------------------------|--------------------------|----------------------------|---|------------------|
| 4.3 | 1.46 | 52 | 0.0 | - |
| 6.4 | 1.86 | 52 | 0.0 | - |
| 7.3 | 1.99 | 74 | .0007±.0001 | 7.26 |
| 9.0 | 2.20 | 52 | 0.0 | - |
| 10.2 | 2.32 | 85 | .015±.004 | 4.20 |
| 12.5 | 2.53 | 52 | .022±.002 | 3.82 |
| 13.0 | 2.56 | 86 | .044±.004 | 3.12 |
| 16.0 | 2.77 | 78 | .066±.006 | 2.72 |
| 17.5 | 2.86 | 73 | .052±.005 | 2.96 |

This data is graphed in figures 29 and 30. Figure 29 yields a reaction threshold power of 10±1 watts. Figure 30 has a slope of 2.6±.7

Pyrolysis Reaction Rate Study

Hot tube pyrolyses were performed and infrared spectra taken on the products. The 1330 cm⁻¹ peak was measured for each pyrolysis and its absorbance related to the pyrolysis temperature and time. A typical infrared spectrum (#84) for this part of the project is included as figure 25.

Table 5: Pyrolysis Reaction Rate Study

| <u>Pyrolysis Temperature (°C)</u> | <u>Pyrolysis time (min)</u> | <u>Spectrum Number</u> | <u>Absorbance</u> | <u>-ln(Abs)</u> |
|-----------------------------------|-----------------------------|------------------------|-------------------|-----------------|
| 300 | 60 | 75 | 0.0 | - |
| 400 | 60 | 76 | 0.0 | - |
| 450 | 60 | 77 | 0.0 | - |
| 500 | 60 | 79 | .015 | 4.20 |
| 550 | 20 | 81 | .020 | 3.91 |
| 550 | 40 | 81 | .055 | 2.90 |
| 550 | 60 | 80 | .171 | 1.76 |
| 550 | 85 | 84 | .218 | 1.52 |
| | | | .228 | 1.47 |
| 550 | 100 | 83 | .225 | 1.49 |
| | | | .222 | 1.51 |
| 550 | 120 | 82 | .239 | 1.43 |
| | | | .231 | 1.47 |

This data is graphed in figures 26 and 27.

Reaction Temperature Calculation

A computer program was designed by Professor David Peak of the Union College Physics Department to calculate the temperatures in a laser beam passing through a gas in a cylindrical cell. The program was used with a cell length of .1 m, a cell radius of .011 m, and a beam radius of .002 m. The thermal conductivity of freon 113 used was .1000 J/cm²sec(°C/cm). 20 temperatures were calculated along the length of the cell (every 5 mm.) The average

absorptivity $M = \ln(P'/P'')/(\text{cell length})$ and the average temperature in the first quarter of the cell were calculated for all of the irradiations, giving the following data:

Table 6: Calculated Reaction Temperatures

| <u>Irradiation Wavelength ()</u> | <u>P_A (w)</u> | <u>M (cm⁻¹)</u> | <u>T (°C)</u> | <u>Initial Reaction Rate (min⁻¹)</u> |
|-----------------------------------|--------------------------|----------------------------|---------------|---|
| 9.7533 | 10.9 | 17.1 | 600 | .013±.007 |
| 9.7335 | 13.8 | 16.4 | 740 | .012±.002 |
| 9.7335 | 12.7 | 17.7 | 700 | .011±.004 |
| 9.7140 | 12.5 | 16.8 | 680 | .022±.002 |
| 9.7140 | 12.5 | 17.5 | 690 | .024±.003 |
| 9.6948 | 12.8 | 18.0 | 710 | .018±.003 |
| 9.6760 | 12.0 | 15.1 | 630 | .0106±.0006 |
| 9.6574 | 11.6 | 14.1 | 590 | .0033±.0003 |
| 9.6036 | 13.0 | 14.5 | 670 | 0.0 |
| Power Study: | | | | |
| 9.7140 | 4.3 | 16.4 | 250 | 0.0 |
| | 6.4 | 18.1 | 370 | 0.0 |
| | 7.3 | 18.8 | 420 | .0007±.0001 |
| | 9.0 | 18.9 | 520 | 0.0 |
| | 10.2 | 14.3 | 530 | .015±.004 |
| | 12.5 | 16.8 | 630 | .022±.002 |
| | 13.0 | 13.8 | 660 | .044±.004 |
| | 16.0 | 17.1 | 870 | .066±.006 |
| | 17.5 | 14.8 | 900 | .052±.005 |

Figure 9: Power Out Vs. Power Into Cell Window

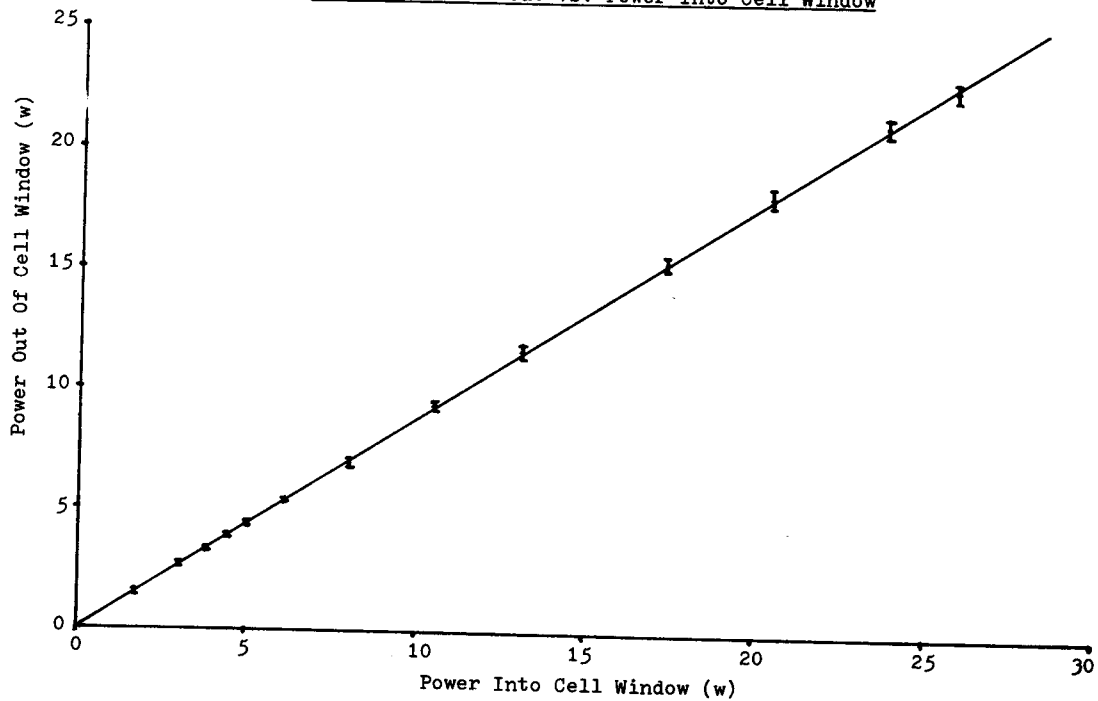


Figure 10: Power 10 cm Back Vs. Power Into Cell Window

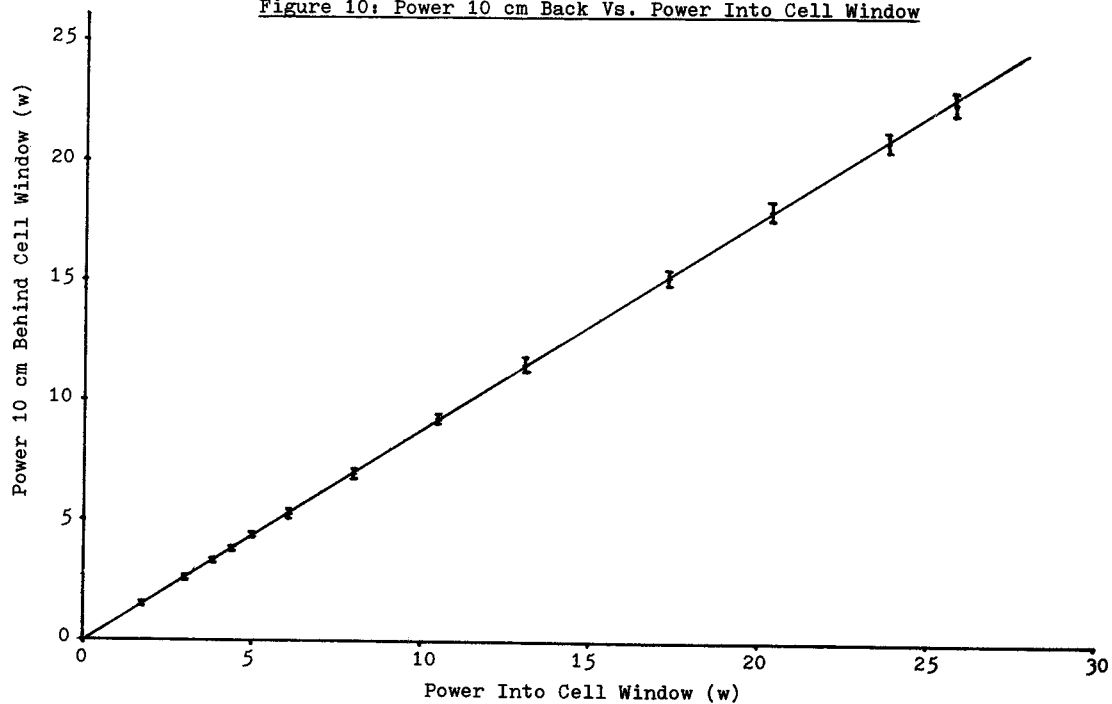


Figure 11A: Infrared Spectrum of a Laser Induced Reaction

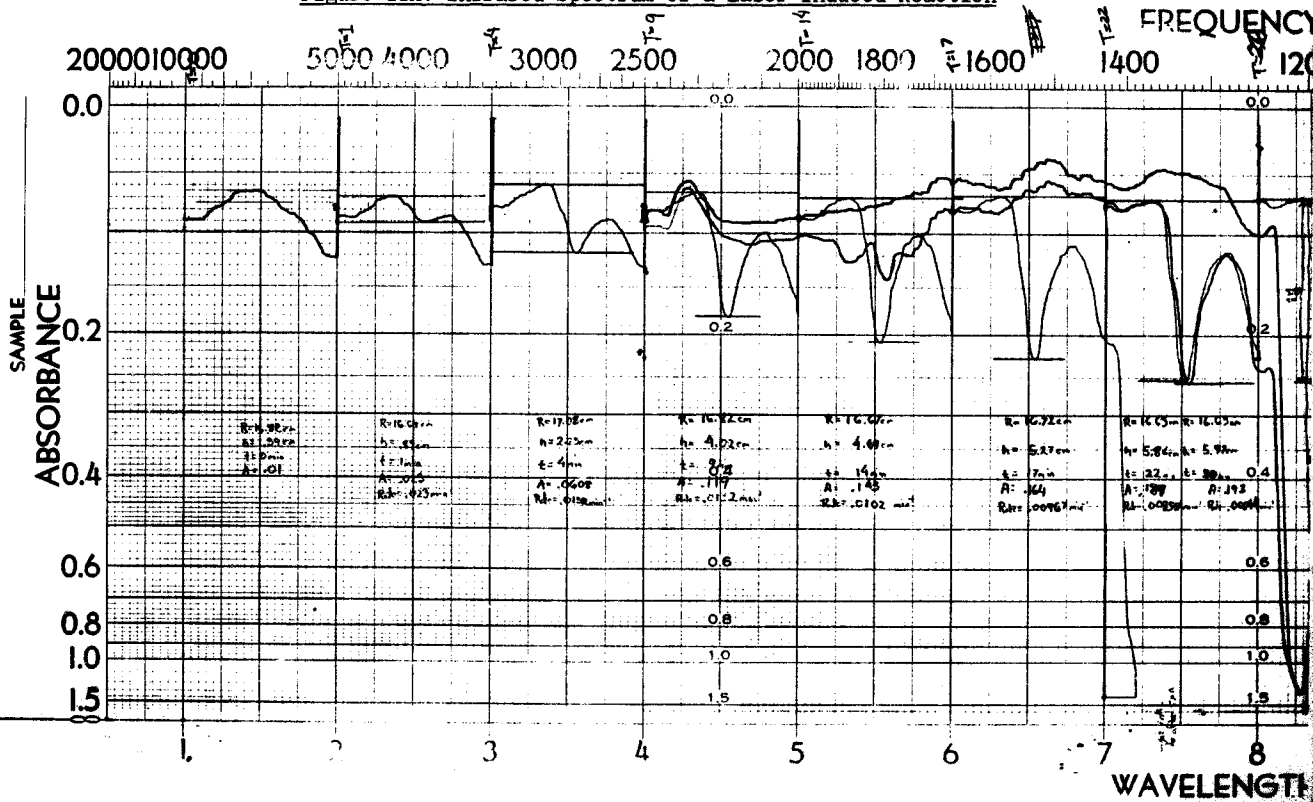
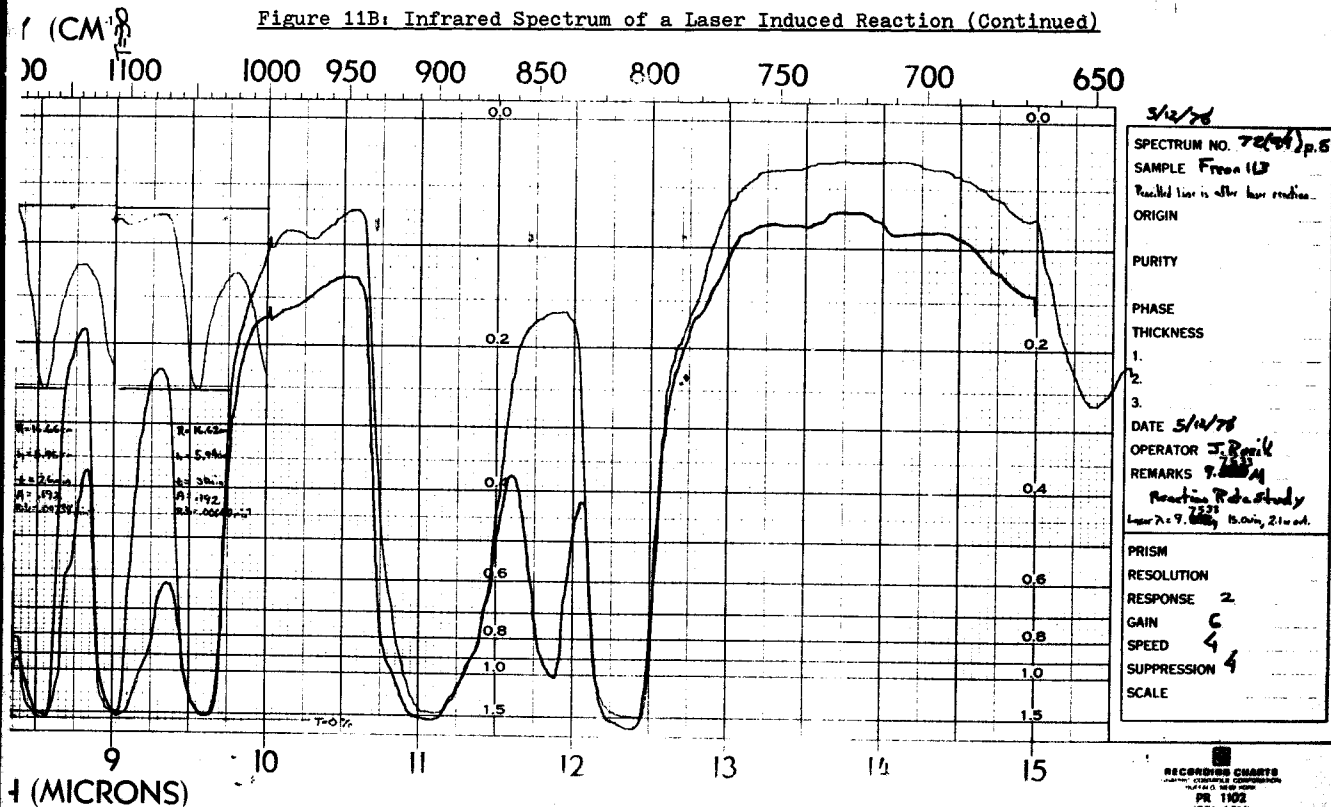


Figure 11B: Infrared Spectrum of a Laser Induced Reaction (Continued)



5/2/78

SPECTRUM NO. 70(4) P. 6

SAMPLE FROM (LB)

Reacted line is after laser reaction.

ORIGIN

PURITY

PHASE

THICKNESS

1.

2.

3.

DATE 5/14/78

OPERATOR J. R. Reilly

REMARKS 9. 10. 11. 12. 13. 14. 15. 16. 17. 18. 19. 20. 21. 22. 23. 24. 25. 26. 27. 28. 29. 30.

Reaction Rate Study

Laser 70. 75. 80. 85. 90. 95. 100. 105. 110. 115. 120. 125. 130. 135. 140. 145. 150. 155. 160. 165. 170. 175. 180. 185. 190. 195. 200. 205. 210. 215. 220. 225. 230. 235. 240. 245. 250. 255. 260. 265. 270. 275. 280. 285. 290. 295. 300. 305. 310. 315. 320. 325. 330. 335. 340. 345. 350. 355. 360. 365. 370. 375. 380. 385. 390. 395. 400. 405. 410. 415. 420. 425. 430. 435. 440. 445. 450. 455. 460. 465. 470. 475. 480. 485. 490. 495. 500. 505. 510. 515. 520. 525. 530. 535. 540. 545. 550. 555. 560. 565. 570. 575. 580. 585. 590. 595. 600. 605. 610. 615. 620. 625. 630. 635. 640. 645. 650. 655. 660. 665. 670. 675. 680. 685. 690. 695. 700. 705. 710. 715. 720. 725. 730. 735. 740. 745. 750. 755. 760. 765. 770. 775. 780. 785. 790. 795. 800. 805. 810. 815. 820. 825. 830. 835. 840. 845. 850. 855. 860. 865. 870. 875. 880. 885. 890. 895. 900. 905. 910. 915. 920. 925. 930. 935. 940. 945. 950. 955. 960. 965. 970. 975. 980. 985. 990. 995. 1000.

PRISM

RESOLUTION

RESPONSE 2

GAIN C

SPEED 4

SUPPRESSION 4

SCALE

Figure 12: Absorbance Vs. Time at 9.7533 μ

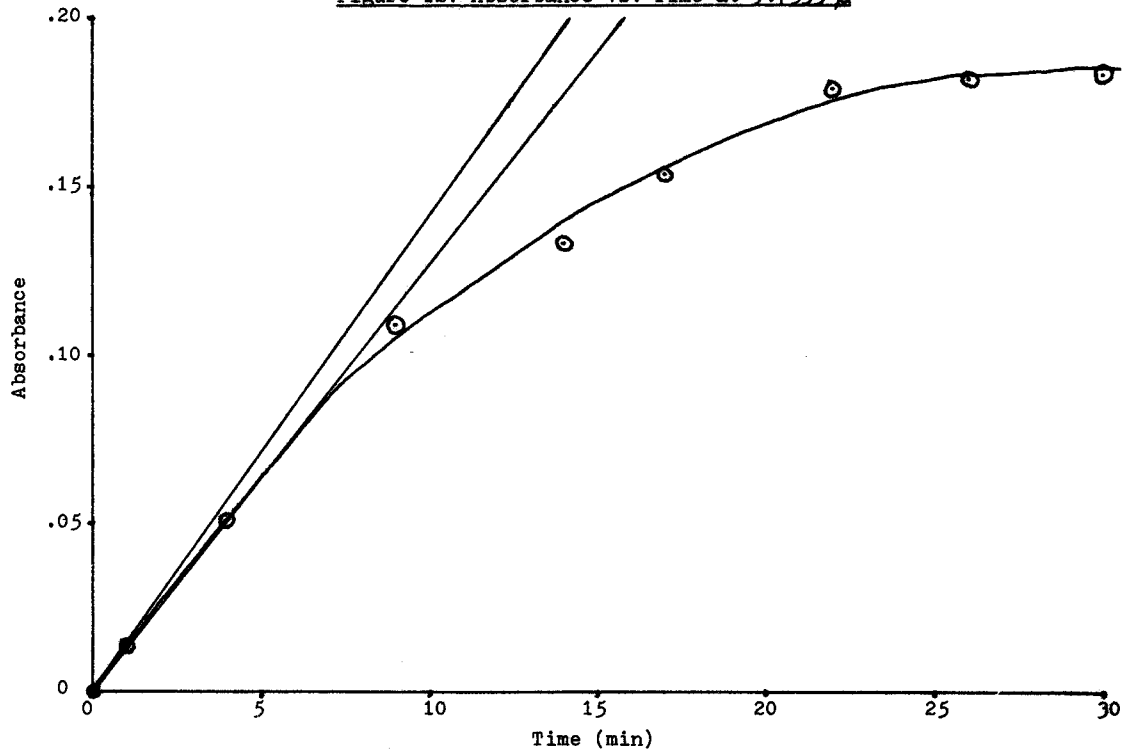


Figure 13: Absorbance Vs. Time at $9.7335\ \mu$

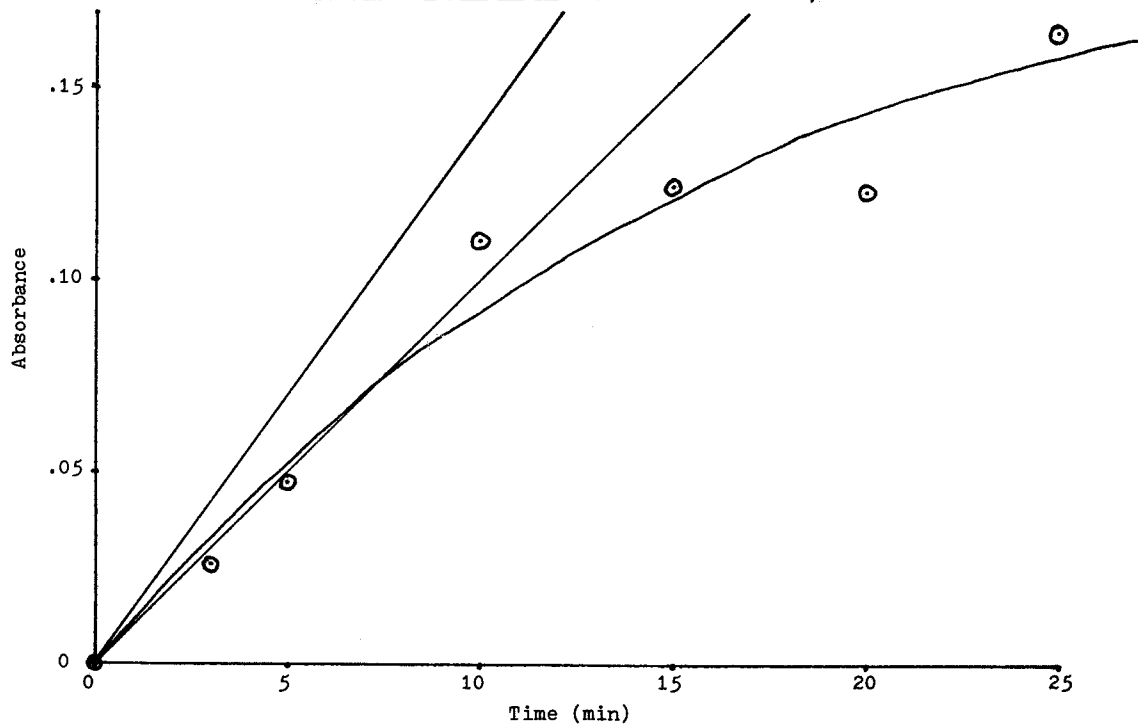


Figure 14: Absorbance Vs. Time at 9.7335 μ

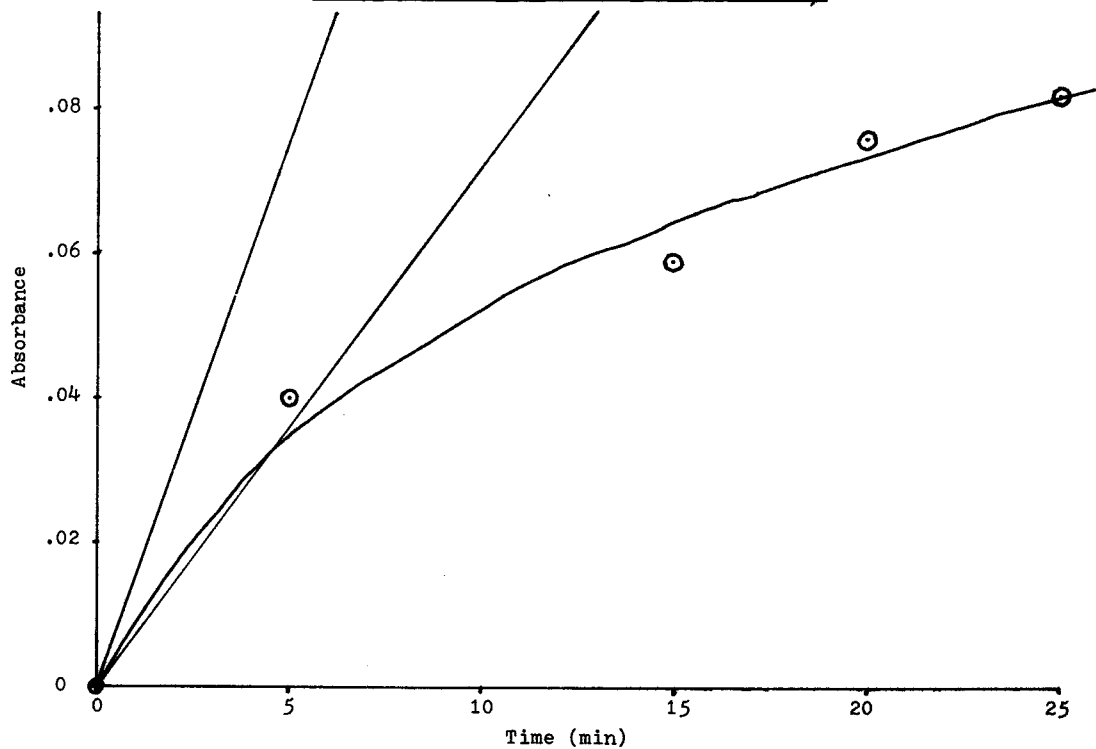


Figure 15: Absorbance Vs. Time at 9.7140 μ

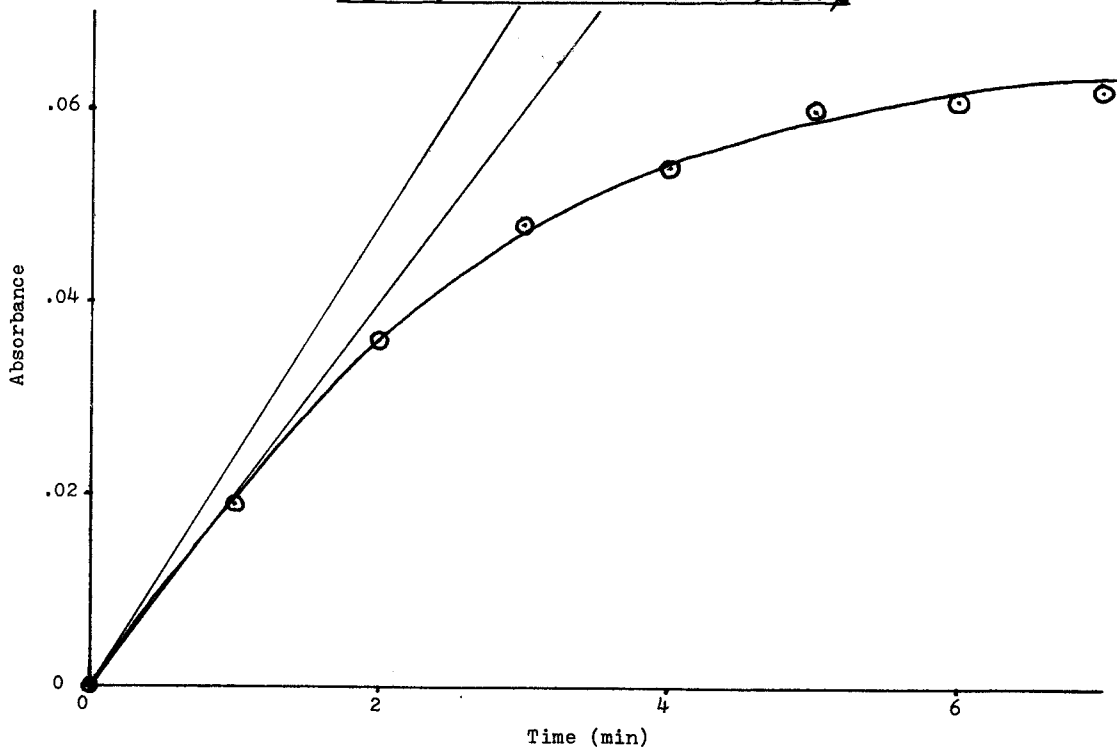


Figure 16: Absorbance Vs. Time at 9.7140 μ

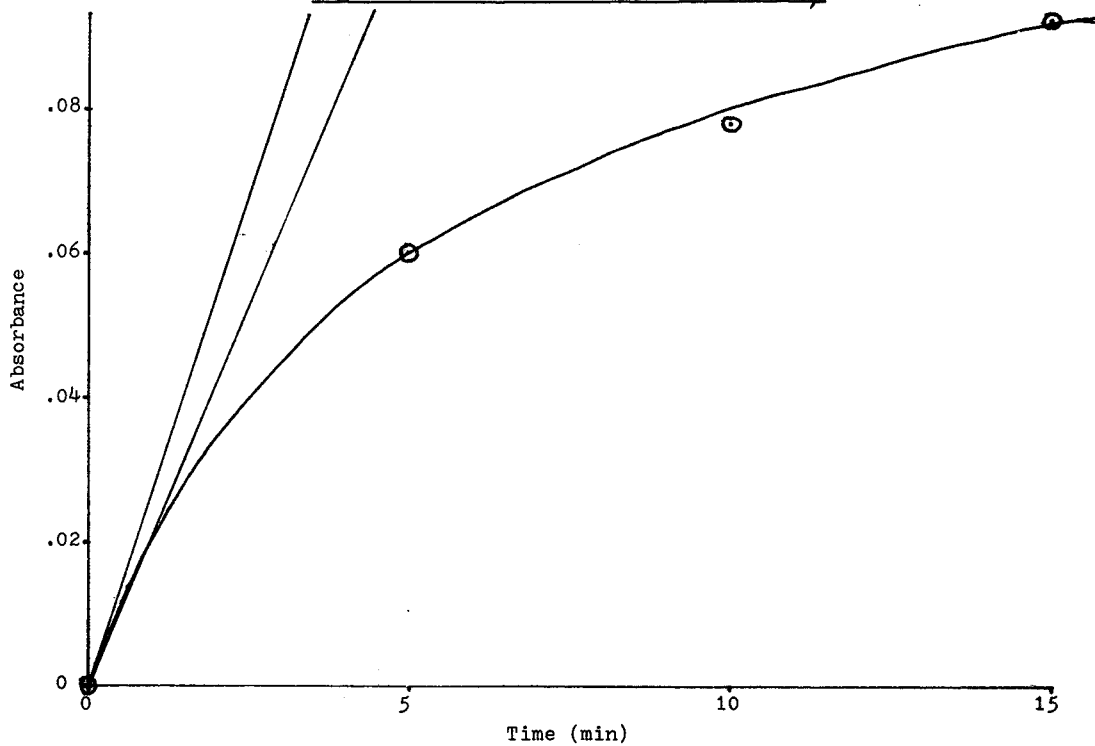


Figure 17: Absorbance Vs. Time at 9.6948 μ

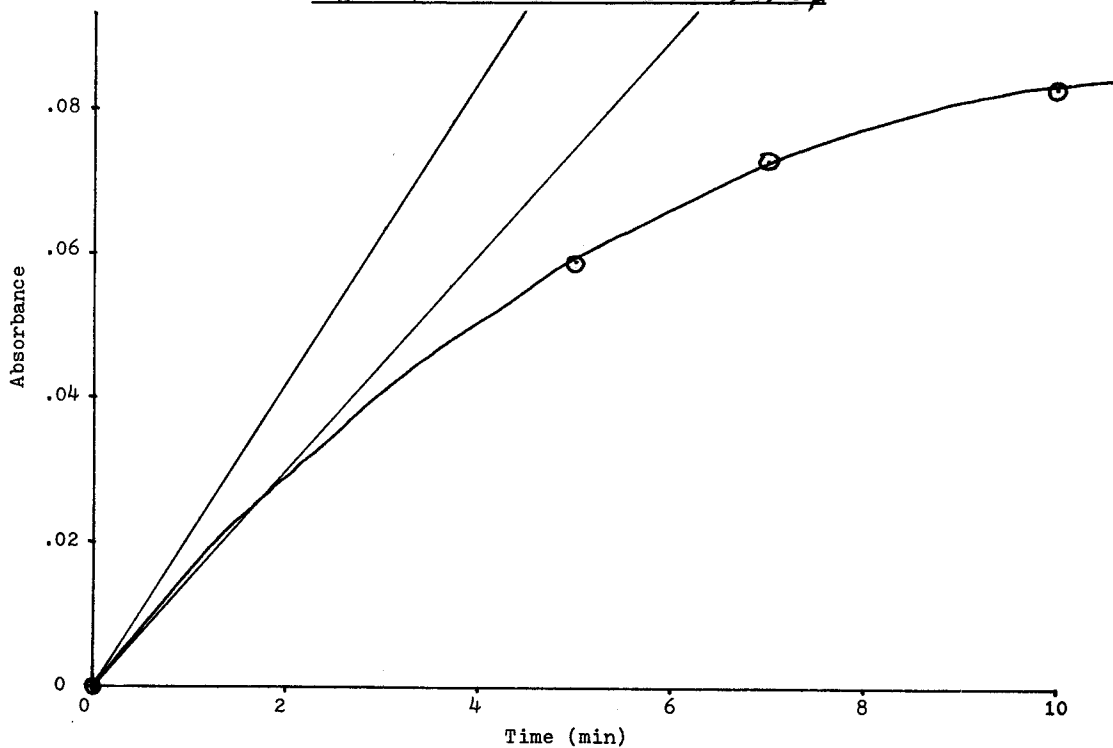


Figure 18: Absorbance Vs. Time at 9.6760 μ

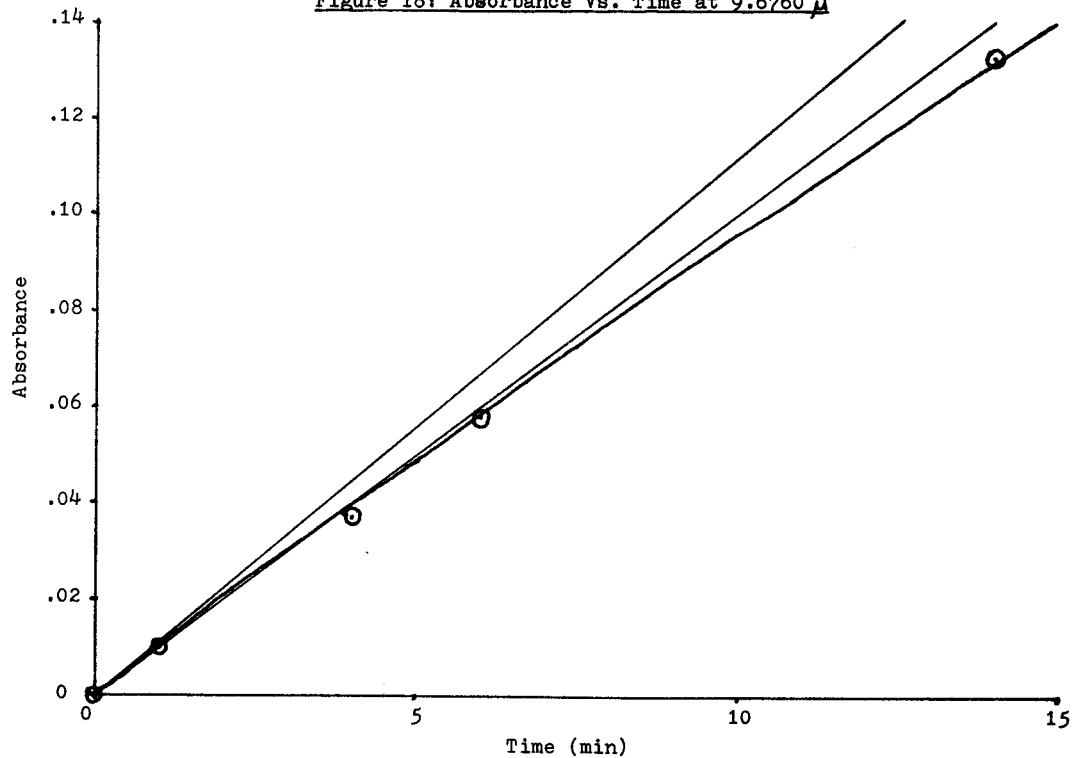


Figure 19: Absorbance Vs. Time at 9.6574μ

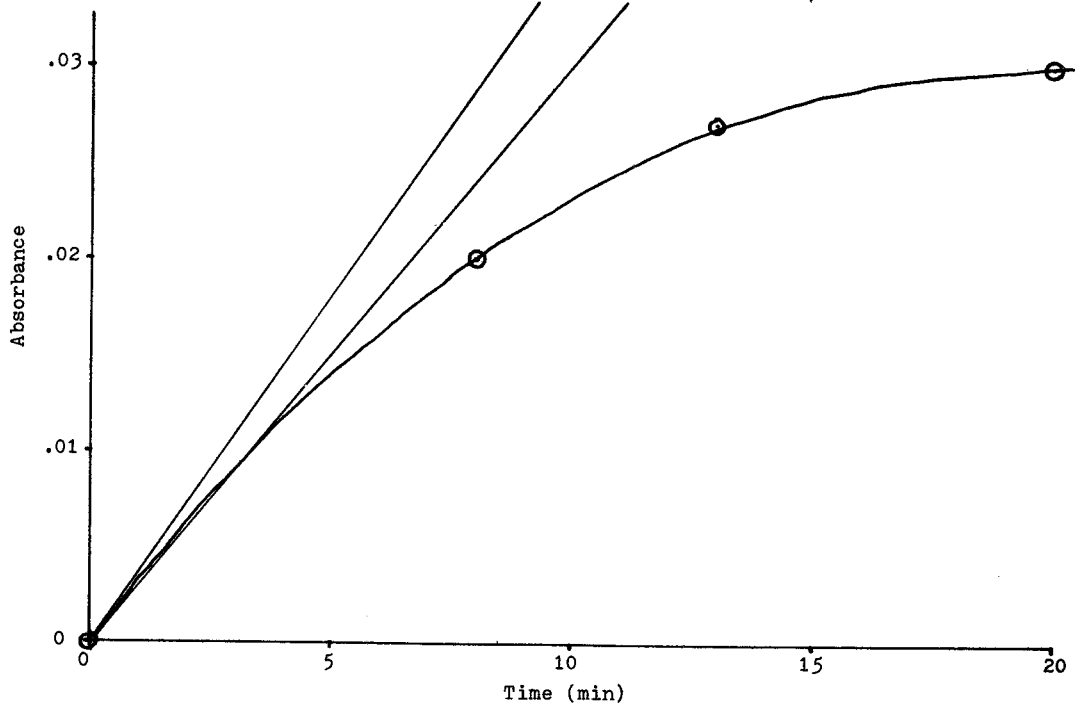


Figure 20: Absorbance Vs. Time at 7.3 w

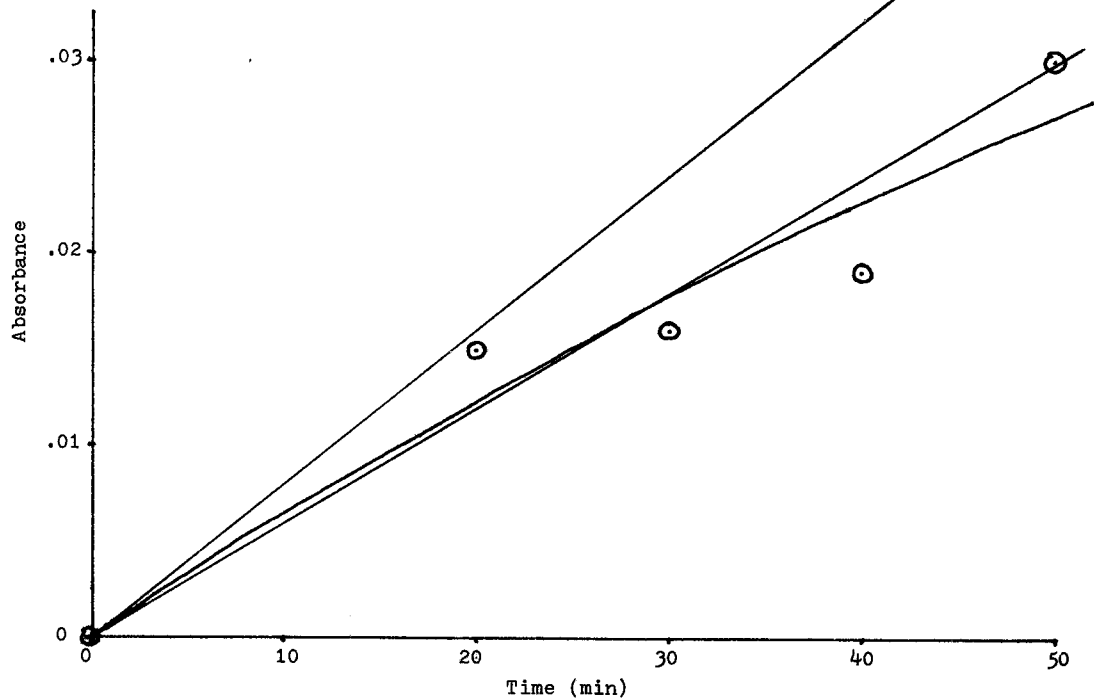


Figure 21: Absorbance Vs. Time at 10.2 w

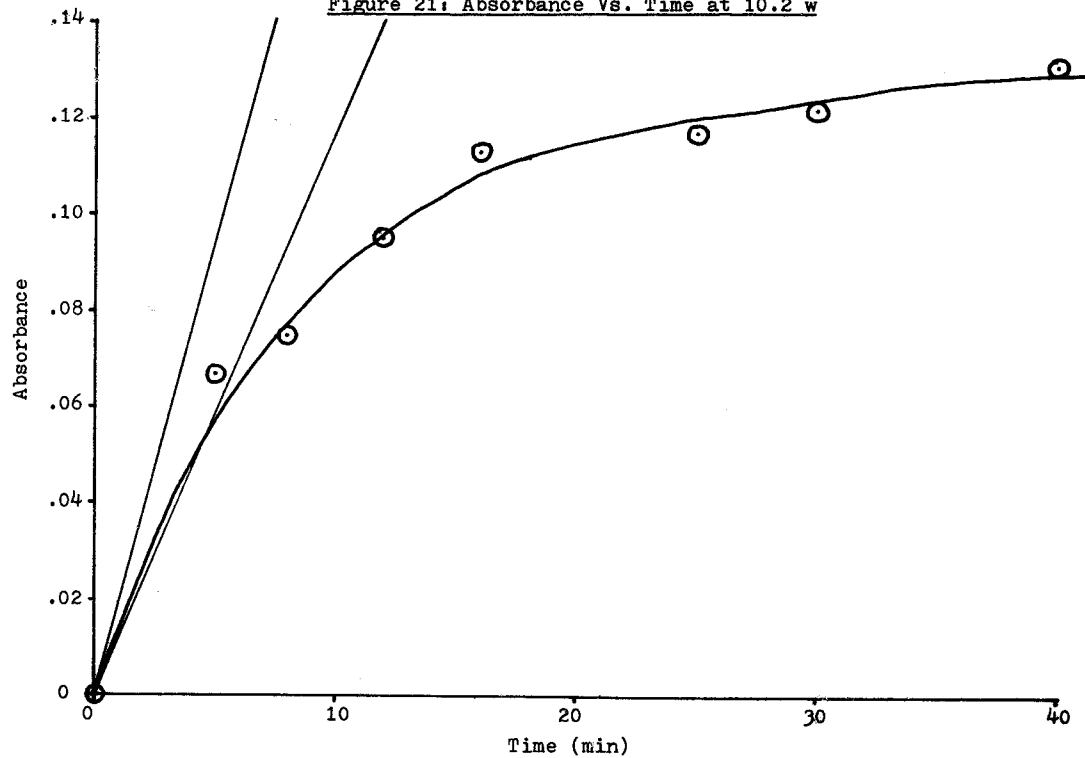


Figure 22: Absorbance Vs. Time at 13.0 w

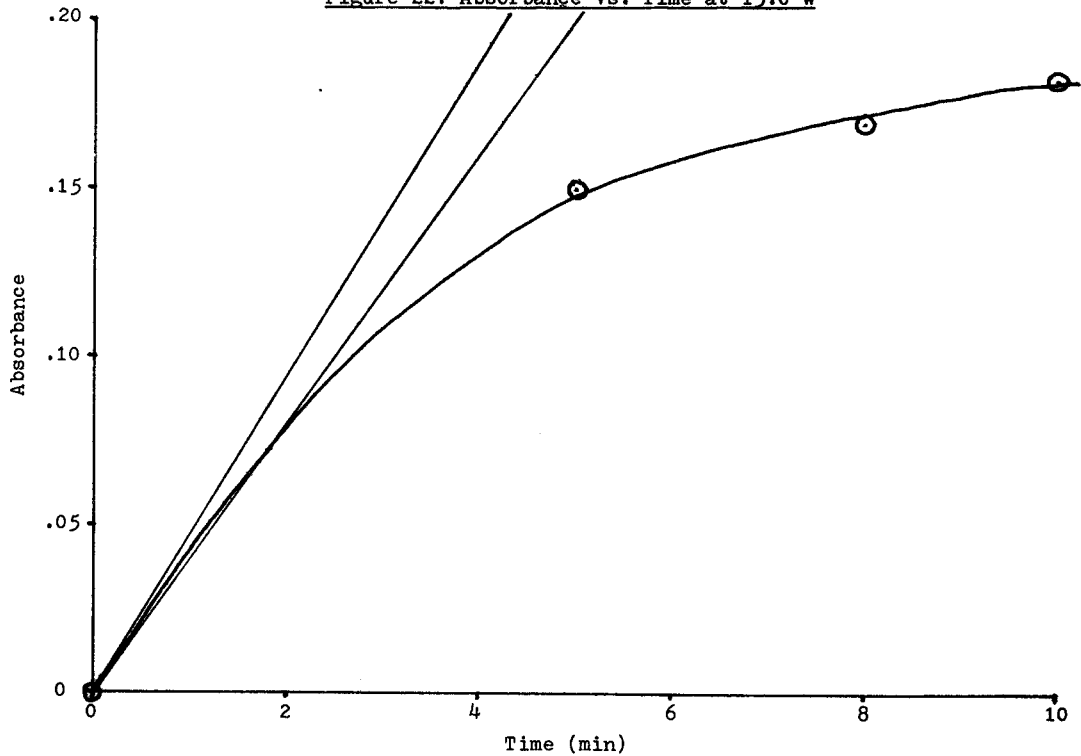


Figure 23: Absorbance Vs. Time at 16.0 w

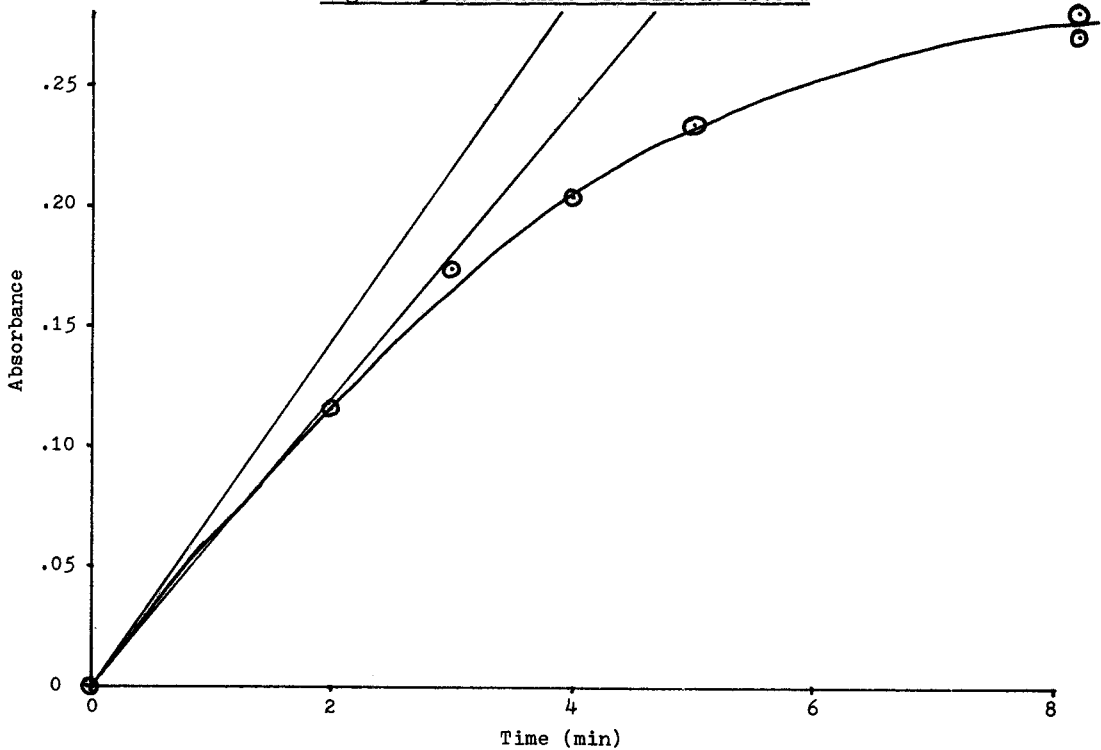


Figure 24: Absorbance Vs. Time at 17.5 w

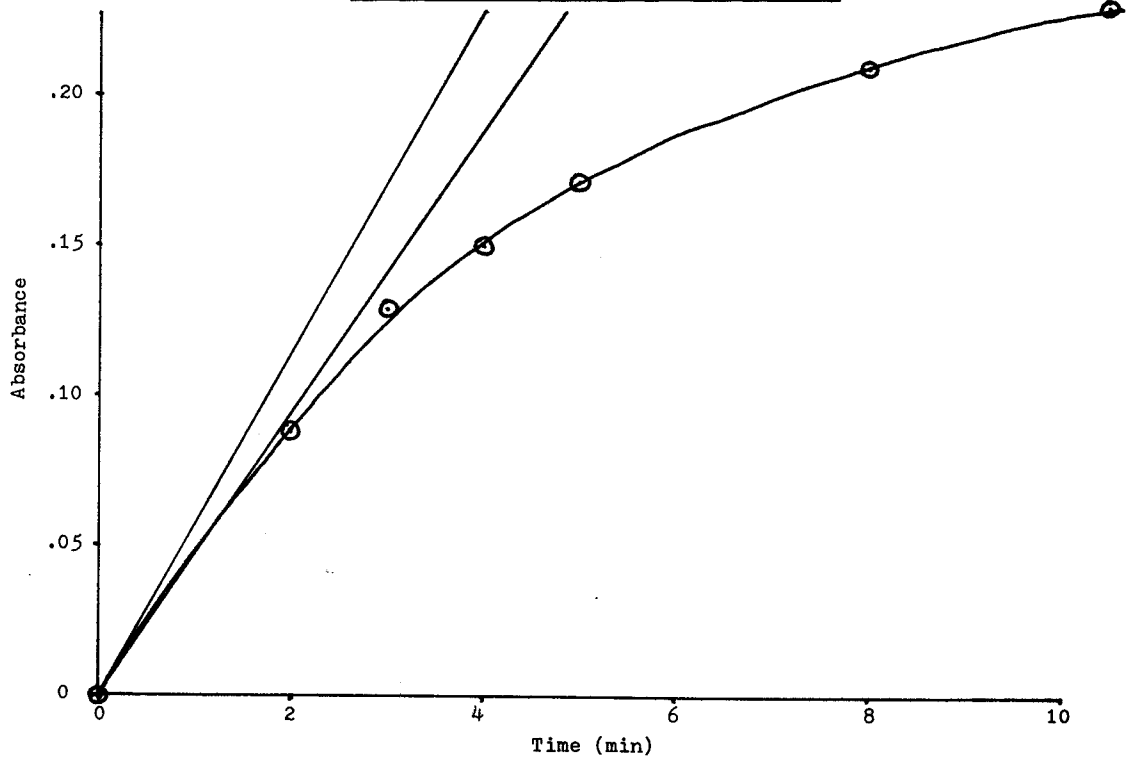
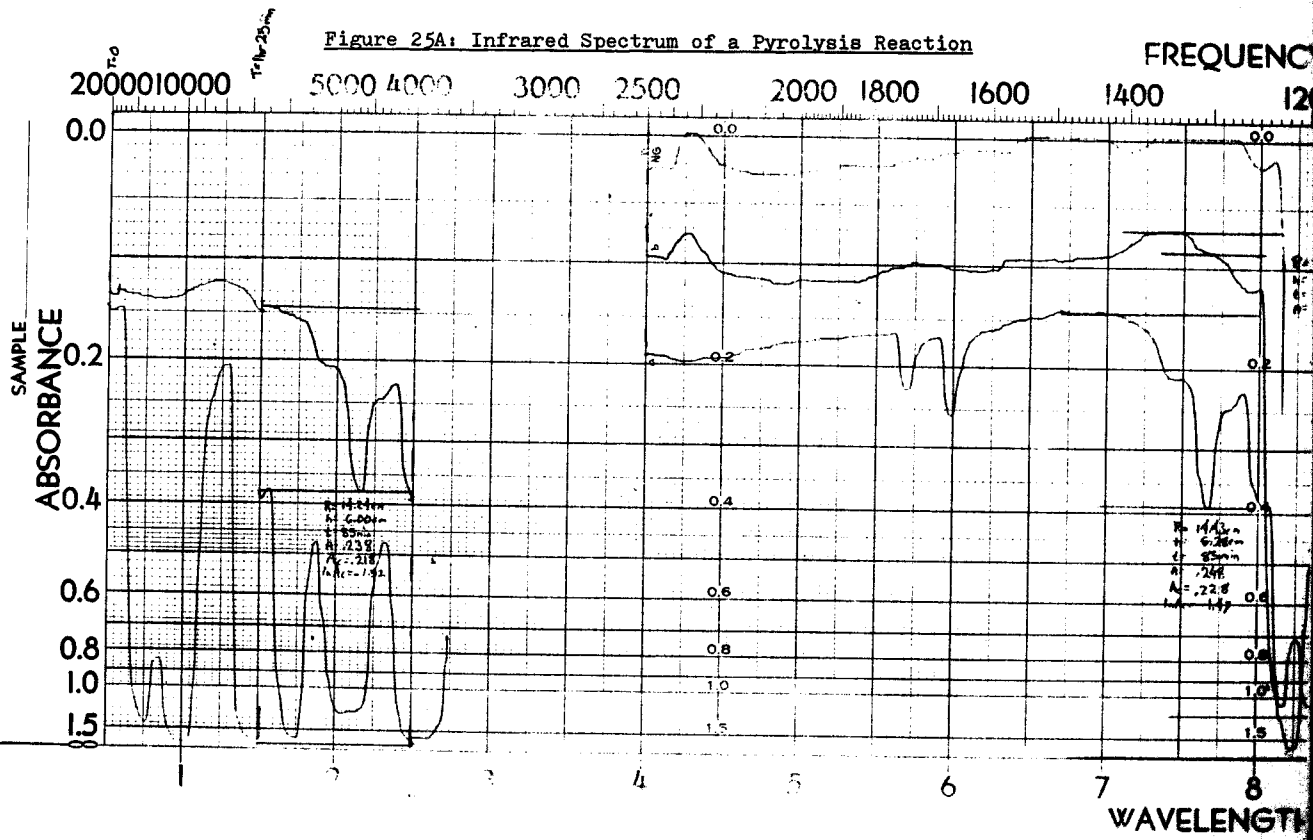


Figure 25A: Infrared Spectrum of a Pyrolysis Reaction



Y (CM⁻¹)

100

1100

1000 950

900

850

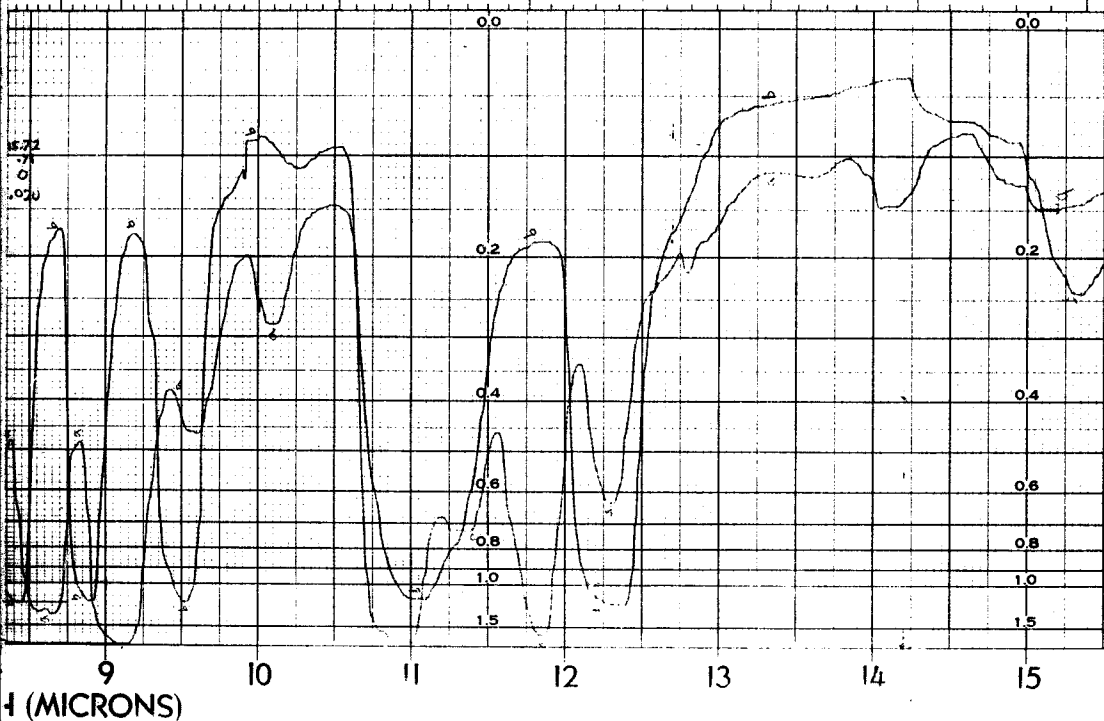
800

750

700

650

Figure 25B: Infrared Spectrum of a Pyrolysis Reaction (Continued)



SPECTRUM NO. 84 p 44
 SAMPLE From 113 of Pyrolysis Plate
 550°C for 1 hr 25 min
 ORIGIN
 PURITY
 PHASE
 THICKNESS
 1.
 2.
 3.
 DATE 5/20/79
 OPERATOR J. Rank
 REMARKS b is before pyrolysis,
 a is after
 PRISM
 RESOLUTION
 RESPONSE 2
 GAIN C
 SPEED 4
 SUPPRESSION C
 SCALE

Figure 26: Absorbance Vs. Time for Pyrolysis

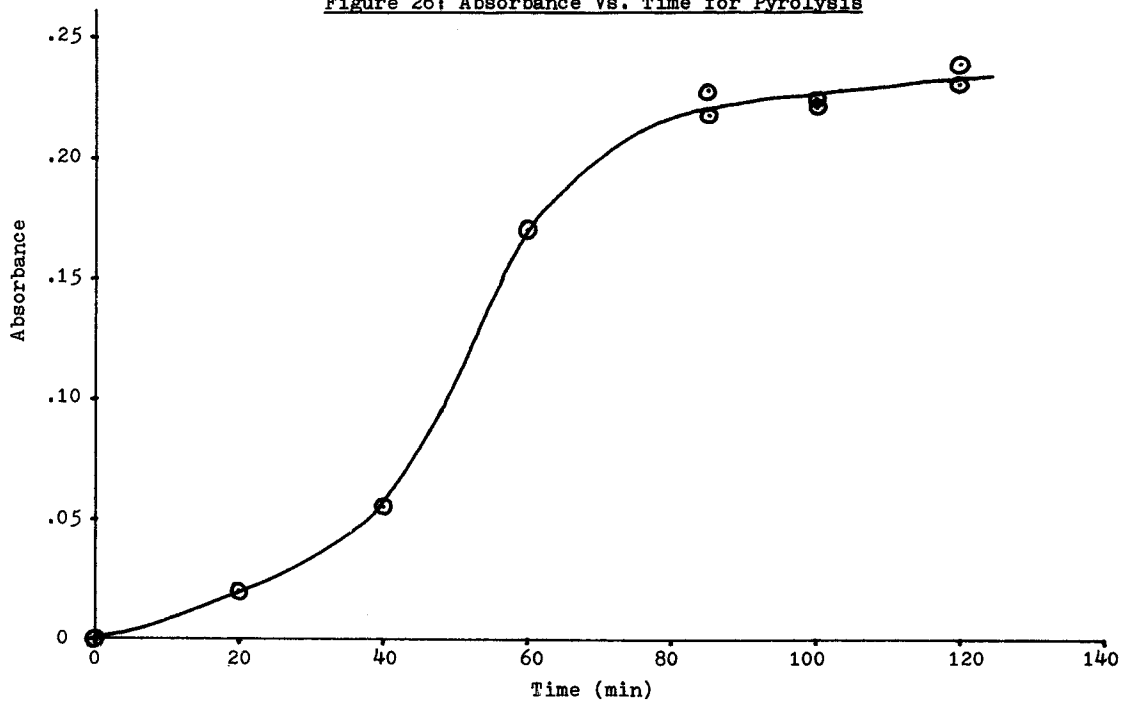


Figure 27: $-\ln(\text{Absorbance})$ Vs. Time for Pyrolysis

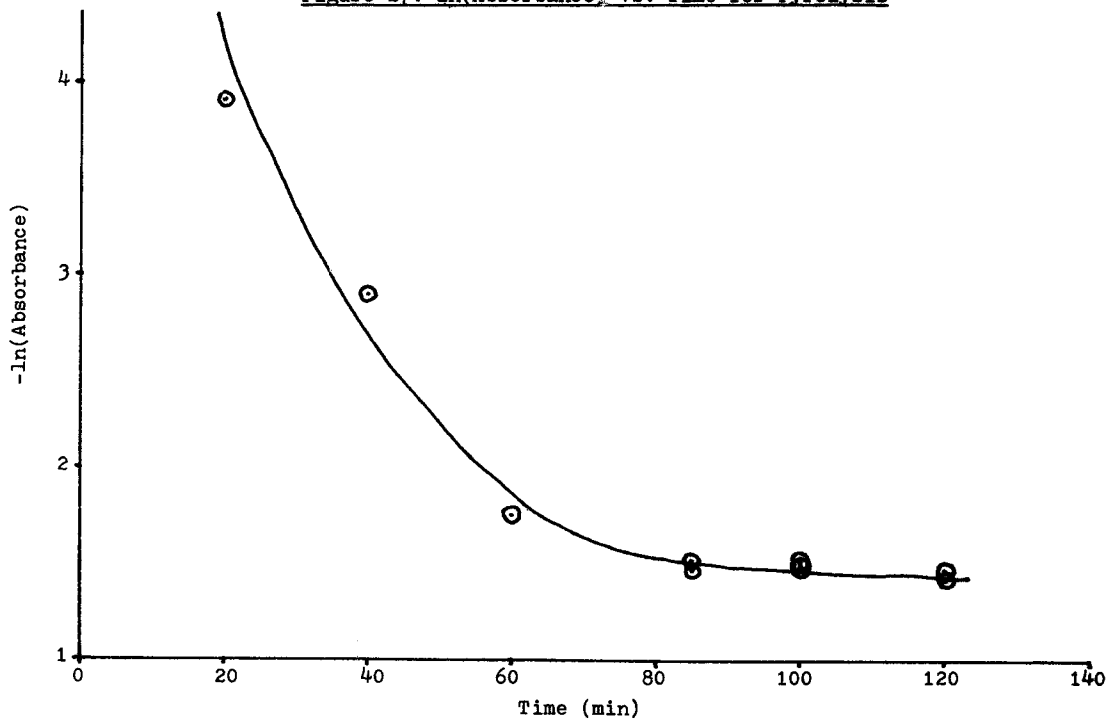


Figure 28: Initial Reaction Rate Vs. Irradiation Wavelength

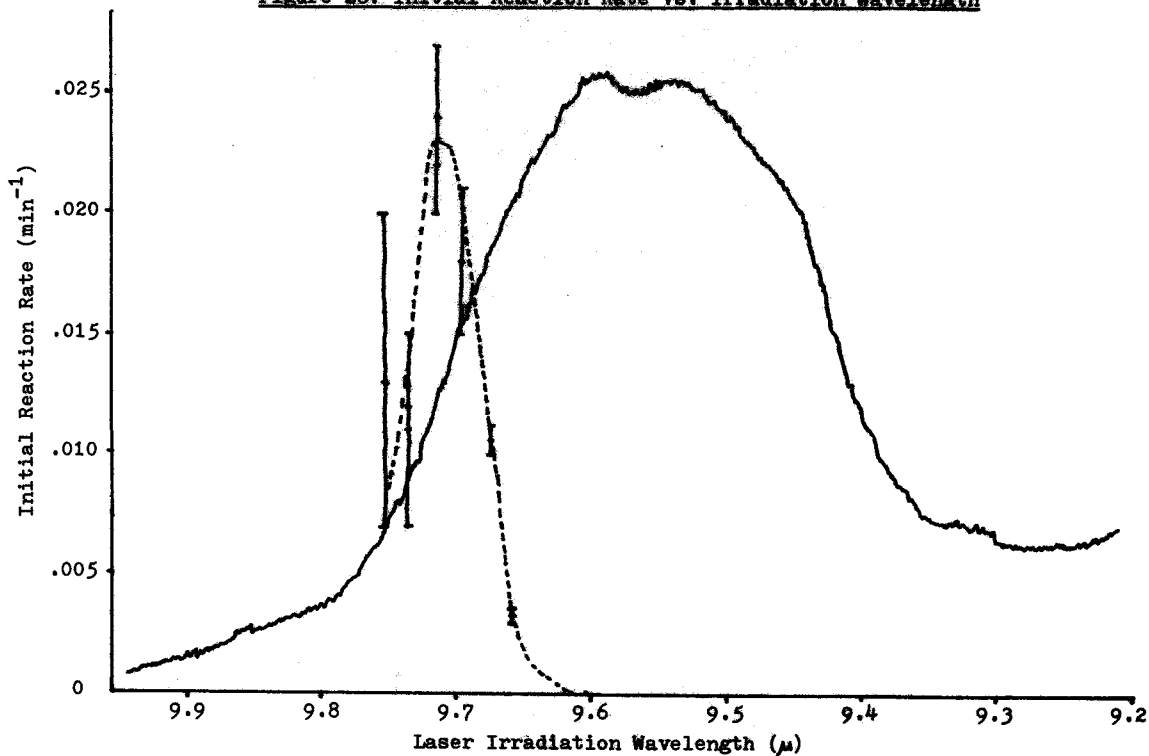


Figure 29: Absorbed Power Vs. Initial Reaction Rate at 9.7140 μ

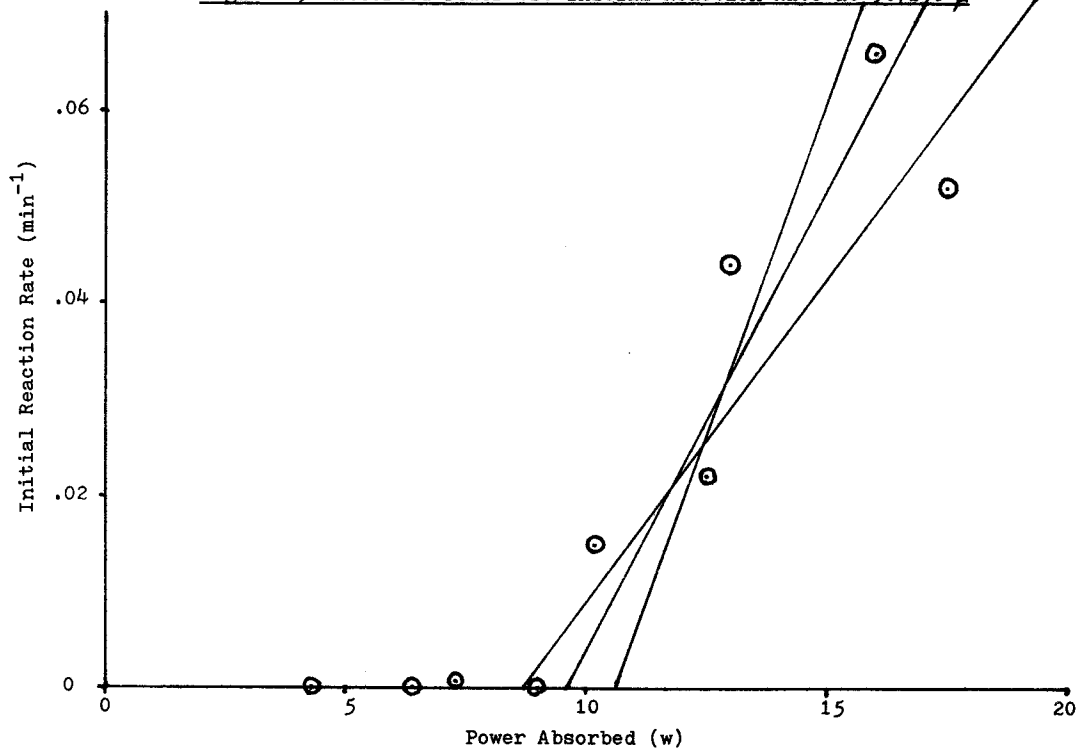


Figure 30: $-\ln(\text{Initial Rate})$ Vs. $\ln(\text{Power Absorbed})$ at 9.7140μ

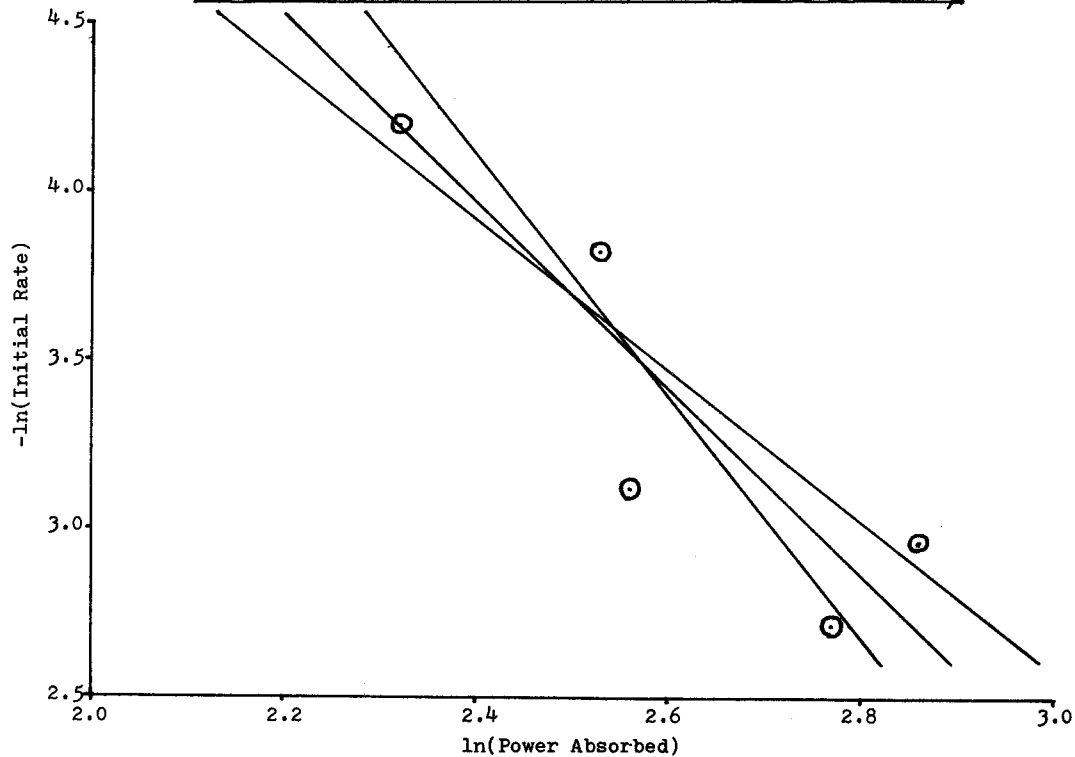
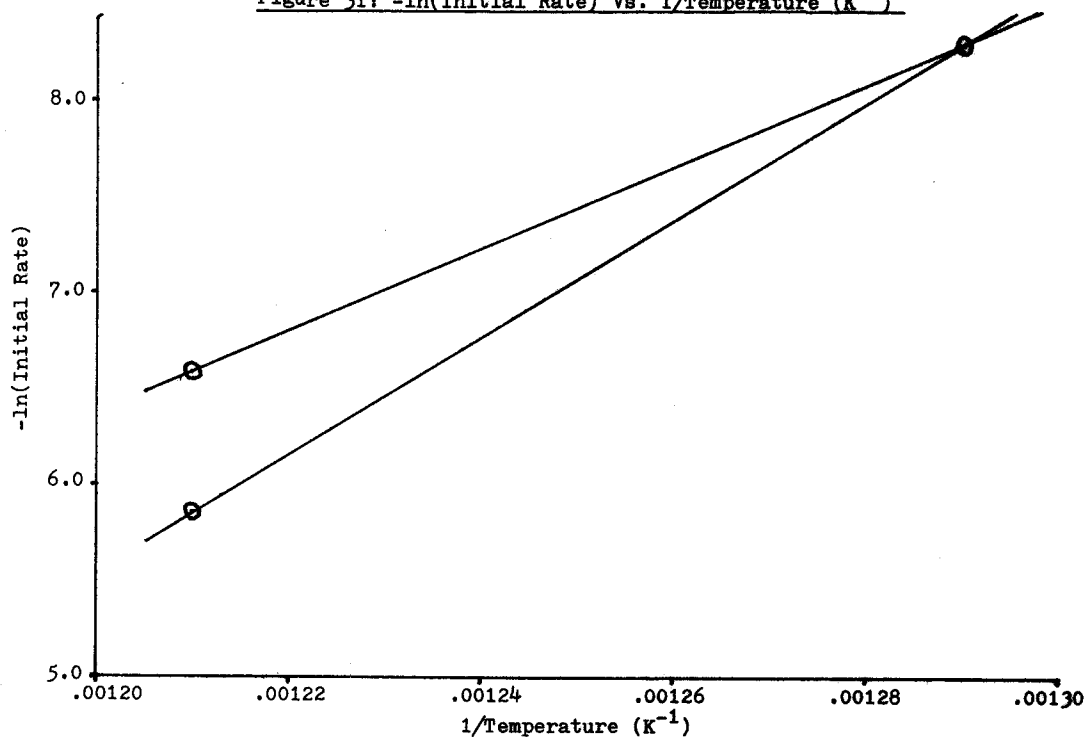


Figure 31: $-\ln(\text{Initial Rate})$ Vs. $1/\text{Temperature (K}^{-1}\text{)}$



Discussion

The Perkin Elmer 21 Infrared Spectrophotometer was particularly useful for this project. Its prism optics give infrared spectra with a linear dependence on wavelength rather than frequency. This results in an expansion of the long wavelength portion of the spectrum relative to instruments with diffraction grating optics, and most of the infrared peaks associated with freon 113 and its reaction products are found in this region.

The infrared spectra (figure 11) taken before, during, and after the laser irradiations show the progress of the resultant chemical reactions. Four clearly detectable absorption peaks are formed which are attributable to products of the laser induced reaction: two small peaks at 1880 cm^{-1} and 1795 cm^{-1} , the moderate peak at 1330 cm^{-1} which was monitored for product formation, and a strong peak at 845 cm^{-1} . Curtis Brown has identified CCl_2F_2 , CClF_3 , and CCl_3F as reaction products by gas chromatography.²⁴ The product peaks at 1330 cm^{-1} and 1795 cm^{-1} have been attributed to chlorotrifluoroethylene²⁵ and the peak at 845 cm^{-1} to trichlorofluoromethane²⁶ by comparison to infrared spectra in literature.

Richard Herrick has shown that the chlorotrifluoroethylene formation due to laser irradiation initially follows zero order kinetics.²² The absorbance of the

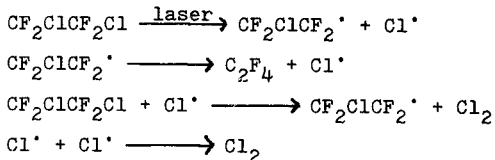
product peak is linear with respect to time at low time values. The kinetic plots for this project (figures 12-24) also suggest this relationship. At later times, however, the slope of the absorbance versus time graph decreases. This is probably due to the decomposition or further reaction of the chlorotrifluoroethylene product when its partial pressure in the reaction mixture becomes significant.

The vibrational stimulation of a chemical bond should logically promote homologous cleavage of that bond, giving rise to free radicals. Obviously with a reactant such as freon 113 the resultant reaction mechanism could be extremely complicated. This is why initial product formation rates were used.

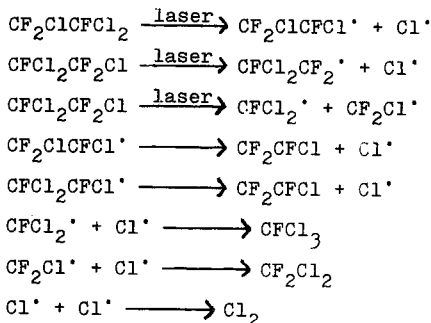
The C-C stretch of freon 113 does not appear in its infrared spectrum because of interference with the intense peaks which surround it. This C-C stretching vibration would appear in the $1200-800\text{ cm}^{-1}$ region, however.²⁷ This could easily cause this vibrational mode to couple strongly with the C-Cl bond stretch being stimulated by the laser. The intramolecular exchange of energy between various vibrational degrees of freedom is usually very rapid in the presence of quasi-resonance between these vibrational modes.⁷ This vibrational stimulation of the C-C bond could explain the presence of single carbon products. It is unfortunate that the growth of the trichlorofluoromethane product peak at 845 cm^{-1} is difficult to monitor because of

the neighboring peaks. The characterization of a single carbon product formation could give much insight into this intramolecular energy transfer.

Zitter and Koster have proposed the following mechanism for the laser induced decomposition of 1,2 dichlorotetrafluoroethane:²⁸



By applying this mechanism to freon 113 and taking into account the C-C vibrational stimulation possible, the following mechanism may characterize the laser induced reaction of freon 113:



The spectrum of the pyrolysis products (figure 25) is clearly different from that of the laser induced reaction products. The product peaks include the 1795 cm^{-1} and 1330 cm^{-1} chlorotrifluoroethylene peaks, a very strong

845 cm^{-1} trichlorofluoromethane peak, and an overtone at 1670 cm^{-1} . In addition there is a product peak at 990 cm^{-1} (moderate,) 880 cm^{-1} (weak,) and 710 cm^{-1} (weak.) The freon 113 peaks at 1040 cm^{-1} and 810 cm^{-1} became significantly smaller with the pyrolysis. This probably indicates that a large portion of the freon 113 has reacted, as the very strong single carbon product peak also suggests. The chlorotrifluoroethylene product peak is not very intense for these conditions, which again suggests decomposition of this product.

Some of the differences between the pyrolysis and laser induced product spectra can be explained by the experimental conditions. The graph of $\ln(\text{absorbance})$ versus time (figure 27) clearly shows that the pyrolysis formation of chlorotrifluoroethylene does not follow first order reaction kinetics. The absorbance versus time graph (figure 26) is very similar to the corresponding laser induced product formation plot, with the exception of an initiation period. This is due at least in part to the time necessary to bring the cell to thermal equilibrium. Another factor is the thermal decomposition of the product, which is given more time to occur than in the laser induced reaction.

The pyrolysis apparently favors the formation of trichlorofluoromethane (and other products) to that of chlorotrifluoro ethylene when compared to the laser induced reaction. A possible explanation is that the laser stimulation in-

creases the rate constants of one or more of the steps in the free radical mechanism. It is extremely unlikely that all of the differences between the two reactions can be explained by the time or temperature differences. This suggests that the thermal reaction model is not applicable to the laser induced reaction.

At an irradiation wavelength of 9.6036μ , 13.0 watts of power are absorbed but no reaction is observed. At 9.7533μ only 10.9 watts are absorbed and reaction occurs. The thermal model for the laser induced reaction predicts that the reaction rate will be greater for the 13.0 watt absorption. It is clear that this reaction cannot be totally explained with only thermal considerations, although it may still be helpful to consider the temperatures produced by the laser. With a continuous wave laser it is difficult to be certain that even miniscule power absorption does not result in a moderate translational temperature increase.²⁹

When the laser radiation is absorbed as vibrational energy, in a relatively short time this energy is thermalized by collisions. Thermal energy is accumulated in the reaction zone, creating a temperature gradient at its boundaries. Thermal diffusion then takes place, and a steady state is reached when this diffusion balances the production of thermal energy in the reaction zone.¹⁰ A theoretical model along these lines was developed by Peak and co-

workers. (See appendix.) A computer program was developed which calculated the temperatures in the center of a laser beam as a function of power intensities and cell dimensions. This program uses the thermal conductivity of the gas and the power absorbed to calculate the temperatures which result from the steady state of diffusion and thermalization. This program is included in the appendix.

In the course of this project, the program format was modified to be more understandable, to include the cell window power absorption, and to calculate the temperatures in degrees Celcius. This program is quite sensitive to radius changes, and as the irradiation cell is not cylindrical it is difficult to determine what value to use for the cell radius. It was assumed that most of the reaction takes place in the first quarter of the cell, as this is where the temperature is the highest and the most power is absorbed. (The first 5 of the 20 temperature values were averaged to get the values listed.) The radius value of .011 m is roughly the average radius for this portion of the cell. Maximum temperatures calculated in this way for laser intensities of 100 w/cm^2 were about 1000°C . Bailey et al reported a similar temperature calculated from fluorescence studies on 40 torr of ethyl chloride with 33 w/cm^2 and a beam diameter of 2.5 cm.³⁰

The laser intensities for this project are not sufficient to excite freon 113 with more than two or three

photons.²² It has been shown that the occurrence of a set of n stepwise single photon absorptions between arbitrary pairs of energy levels results in a slope having a magnitude equal to n when the log of the rate constant is plotted against the log of laser intensity.⁸ The graph of $-\ln(\text{initial rate})$ versus $\ln(\text{power absorbed})$, (figure 30) yields a slope of $2.6 \pm .7$ indicating 2 or 3 photon absorption, or a mixture of both. This is not sufficient to excite freon 113 into the quasi-continuum, however.

Figure 28 shows that the maximum rate of reaction occurs at a longer irradiation wavelength than the maximum absorption peak for the freon. In this case, (freon 113 has a small dipole moment and Stark effect, and low laser intensities were used,) the most plausible explanation is that the laser is not in resonance with the $v=0$ to $v=1$ transition, but rather some higher level transition.

Richard Herrick proposed thermal excitation of the first one or two vibrational states as an explanation.²² The temperature values calculated could easily give significant populations in the $v=1$ and $v=2$ vibrational states. It has been shown that absorption of laser energy by higher level transitions than the ground state is very effective in rate enhancement.³¹ The laser could therefore, for instance, be tuned to the $v=2$ to $v=3$ to $v=4$ transition.

It has been postulated that the quasi-continuum for BCl_3 starts just above its $v=4$ vibrational level, and just

below that level for SF_6 .¹⁵ Because freon 113 has more degrees of freedom than SF_6 , it should have denser vibrational-rotational levels. The quasi-continuum should therefore start at a slightly lower point than for SF_6 , probably just above its $v=3$ vibrational level, which would demand 4 photon excitation. Once in the quasi-continuum the molecule can accept virtually any amount of energy from collisions, where excited molecules not yet in the quasi-continuum can only accept energy in resonance with its vibrational level transitions. This would allow the collisional activation of molecules in the quasi-continuum to much higher energies than those supplied by the laser.³²

Richard Herrick calculated the rate of power absorption to be 7.6×10^2 photons/molecule-sec and the collision rate to be about 10^9 collisions/molecule-sec, thereby proving the importance of collisional activation in this experiment.²² Vibrational-vibrational energy transfer times were compared to Vibrational-rotational/translational energy transfer times for typical molecules, and it was found that there is a good chance for the 20 or more collisional activations (necessary to dissociate a molecule in the quasi-continuum) to occur before thermalization.

This reaction model is called the thermally enhanced photochemical reaction model.²² Similar models have been used by Bailey et al on the laser initiated decomposition of ethyl chloride³⁰ and Zitter and Koster on the laser re-

actions of 1,2 dichlorotetrafluoroethane.²⁸ The reactions produce basically the same products as pyrolyses, but the rates of the reactions (or of selected chain mechanism steps) are enhanced by laser absorption. This model can therefore be called a photocatalytic effect of the laser absorption.³³

The reaction rate dependence on the irradiation wavelength could perhaps be related to the calculated absorptivity (table 6). It seems likely that a higher incident power would be necessary for an equal amount of power to be absorbed off of the reaction rate peak (figure 28). Unfortunately it can be seen in the power study portion of table 6 that the calculated absorptivity varies tremendously. This is probably due to imprecise (although not necessarily inaccurate) power measurements.

The cell window absorption section of this project was introduced as an improvement in power value measuring. The window absorption was previously treated by considering the power absorbed by the irradiation cell with a vacuum. This obviously would assume too much power entering and being absorbed by the back window, and consequentially gave P_A values that were very low.

The plot of initial reaction rate versus power absorbed (figure 29) shows what is known as a threshold phenomenon; an absorbed power (10 ± 1 w) below which no photocatalyzed reaction is possible. The reaction detected at 7.3 w absorbed is probably due totally to laser heating of the cell over 50

minutes. The experimental observation of threshold phenomena has been interpreted by Oraevsky and Pankratov to be theoretically due to the participation of more than just one particular mode of vibration in the absorption of laser radiation.¹⁹ This model would take intramolecular vibrational mode coupling into account in addition to predicting small effects on all vibrational-rotational degrees of freedom. This further justifies the proposed freon 113 laser reaction mechanism by including the C-C cleavage possibility.

An alternative way to look at the reaction rate power dependence is to consider the calculated temperatures in table 6. The calculated temperatures around the threshold frequency correspond to the lowest pyrolysis temperature at which reaction was detected. A purely thermal explanation would not predict a sharp threshold power, however, but rather a slow rate acceleration.

The graph of $-\ln(\text{rate})$ versus $1/\text{Temperature}$ (figure 31) was included for the pyrolysis to get a rough approximation of the Arrhenius energy of activation. Equation 1 gives:

$$-\ln(k) = E^*/R(1/T) + \ln(A) \quad (\text{Equation 9})$$

If $-\ln(k)$ versus $1/T$ is plotted, the slope divided by R , (1.987 cal/mole-K,) will yield the activation energy for the pyrolysis. Figure 31 gives an Arrhenius activation energy of 50 ± 10 kcal/mole, which is comparable to carbon-chlorine bond energies. ($\text{CH}_3\text{-Cl}$ bond energy is 83 kcal/mole, and substitution would lower this value considerably.³⁴)

In conclusion, it has been found that the low power continuous wave infrared laser induced decomposition of freon 113 is photocatalyzed. Bi- or triphotonic laser absorption is accompanied by thermal and collisional stimulation to initiate a reaction which differs significantly from pyrolysis.

Suggestions for Further Work

The laser induced decomposition of freon 113 is open to many research studies. Basically, future work should be done in obtaining more accurate data, and expanding the study to include such variables as pressure, temperature, and laser beam continuity and radius. It would also be interesting to determine the reaction rate power dependence as a function of irradiation frequency or the wavelength dependence as a function of power absorbed. This would yield a three dimensional graph of reaction rate dependence on power and irradiation frequency, which could help limit the problems of interpreting the power differences in the wavelength dependence data in table three.

The laser induced and pyrolytic decomposition of freon 113 has not been fully characterized. The use of infrared spectra to monitor the reactions was sufficient for the basically qualitative discussion offered here, but the product analysis should be expanded to quantitatively describe the decomposition reactions. The possibility of isotope selective laser induced reaction should also be examined. These analyses could both be performed with a gas chromatograph-mass spectrometer. This instrument would allow the separation and determination of the relative amounts of the components of the reaction mixture and the identification of these components, including the isotopic

product ratios. The information provided could be used to pose a more intensive reaction model and mechanism.

UN82
R955C/1979

RUSIK, J.J.
CHEMISTRY

CO2 LASER INDUCED DECOMPOSITION OF FREON 113
HRS. 3/79 SHT. 2 OF 2



END



Appendix

The following computer program for calculating the temperatures in a laser beam which is passing through a gas in a cylindrical cell was developed by Dr. David Peak and his students for this project. It is in BASIC and was run on a Burroughs B-6805 computer.

DIM T(100)

R=0.02

L=0.1

A1=5

L1=0.1

A=0.0015

M=11

68

```
50 REM IN THIS PROGRAM R IS THE CELL RADIUS, L IS THE CELL LENGTH,
51 REM A1 IS THE TEMPERATURE ACCURACY, L1 IS THE THERMAL CONDUCT-
52 REM TIVITY OF THE GAS, A IS THE BEAM RADIUS, N IS THE NUMBER OF
53 REM TEMPERATURE VALUES TO BE CALCULATED ALONG THE CENTER OF THE
54 REM BEAM, N IS THE COUNTER VARIABLE FOR THE SERIES IN THE
55 REM TEMPERATURE EQUATION, S1 IS THE AMBIENT TEMPERATURE IN
56 REM DEGREES CELCIUS, S IS THE AMBIENT TEMPERATURE IN DEGREES
57 REM KELVIN, I3 IS THE INTENSITY OF THE BEAM ENTERING THE SAMPLE,
58 REM I4 IS THE INTENSITY OF THE BEAM LEAVING THE SAMPLE (THERE
59 REM IS AN OPTION OF USING THE VALUES MEASURED BEFORE AND AFTER
60 REM THE CELL WINDOWS, RESPECTIVELY FOR I3 AND I4), I5 IS THE
61 REM POWER ABSORBED BY THE SAMPLE, M1 IS THE AVERAGE ABSORPTIVITY
62 REM OF THE GAS (CALCULATED FROM THE LOG OF THE INTENSITY RATIO
63 REM DIVIDED BY THE CELL LENGTH), X1 IS THE VOLUME OF THE BEAM,
64 REM X2 IS THE VOLUME OF THE CELL, T AND X3 ARE MODIFICATIONS
65 REM OF THESE VOLUMES FOR USE IN THE CALCULATIONS OF THE BESSEL
66 REM FUNCTION VALUES, I2 I1 K2 AND K1 ARE THE CALCULATED VALUES
67 REM OF THE MODIFIED BESSEL FUNCTIONS WORKING ON THE APPROPRIATE
68 REM VOLUME VALUES, Z IS THE DISTANCE ALONG THE LENGTH OF THE
69 REM CELL WHERE THE TEMPERATURE IS BEING CALCULATED, S4 COUNTS
70 REM THE NUMBER OF TIMES THAT THE SERIES IS EVALUATED IN GROUPS
71 REM OF 5 TIMES FOR CHECKING ON TEMPERATURE CONVERGENCE, D KEEPS
72 REM TRACK OF THE ODD AND EVEN TERMS IN THE SERIES EXPANSION,
73 REM T1 AND T2 ARE PARTS OF THE SERIES BEING EVALUATED, S TAKES
74 REM ON THE VALUE OF THE CALCULATED TEMPERATURE, AND T(I) IS THE
75 REM I' TH TEMPERATURE VALUE AFTER THE CONVERGENCE CHECK.
76 REM ALL LENGTHS AND RADII ARE IN METERS, AND ALL INTENSITIES
77 REM ARE IN WATTS.
```

99 N=1

```
100 PRINT " CURRENTLY, THE CELL RADIUS IS "R" METERS,"
101 PRINT "THE CELL LENGTH IS "L" METERS, THE TEMPERATURE"
102 PRINT "ACCURACY IS "A1" DEGREES, THE THERMAL CONDUCTIVITY"
103 PRINT "IS "L1", THE BEAM RADIUS IS "A" METERS, AND "M"
104 PRINT "TEMPERATURES WILL BE CALCULATED ALONG THE CENTER OF"
105 PRINT "THE CELL. DO YOU WANT TO CHANGE ANY OF THESE PARA-"
106 PRINT "METERS?"
107 INPUT F$
108 IF LEFT(F$,1)="N" THEN 322
109 N=1
110 PRINT "INPUT CELL RADIUS IN METERS"
111 INPUT R
112 PRINT "INPUT CELL LENGTH IN METERS"
113 INPUT L
114 PRINT "INPUT THE TEMPERATURE ACCURACY IN DEGREES"
115 INPUT A1
116 PRINT "INPUT THE NUMBER OF TEMPERATURES DESIRED"
117 INPUT M
118 PRINT "INPUT THE THERMAL CONDUCTIVITY OF THE GAS"
119 INPUT L1
120 PRINT "INPUT THE BEAM RADIUS IN METERS"
121 INPUT A
122 PRINT "INPUT THE AMBIENT TEMPERATURE IN DEGREES CELSIUS"
123 INPUT S1
124 PRINT "INPUT THE ENTERING BEAM INTENSITY IN WATTS"
125 INPUT I3
126 PRINT "DO YOU WANT THIS VALUE TO BE CORRECTED FOR POTASSIUM"
127 PRINT "CHLORIDE WINDOW ABSORPTION, REFLECTION, AND REFRACTION"
128 PRINT "OF THE BEAM?"
```

```

330 INPUT R#
331 IF LEFT(R#,1)="N" THEN 335
332 I3=.004+.887*I3
335 PRINT "INPUT THE LEAVING BEAM INTENSITY IN WATTS"
336 INPUT I4
337 PRINT "DO YOU WANT THIS VALUE CORRECTED?"
338 INPUT S#
339 IF LEFT(S#,1)="N" THEN 365
340 I4=.007+1.139*I4
365 PRINT
370 PRINT
375 PRINT
700 I5=I3-I4
710 PRINT "THE POWER ABSORBED BY THE SAMPLE IS "I5" WATTS, AND"
725 M1=(LOG(I3/I4))/L
730 PRINT "THE AVERAGE ABSORPTIVITY IS "M1
732 PRINT
734 PRINT "*****TEMPERATURES*****"
736 PRINT
750 FOR I=1 TO M
800 S=S1+273.15
850 X1=(N#*3.14159)/L
900 X2=(N#*3.14159)/L
950 IF X2 > 3.75 THEN 1025
975 GOSUB 3000
1000 GO TO 1050
1025 GOSUB 3350
1050 IF X2>2 THEN 1120
1075 GOSUB 4600
1100 GO TO 1125
1120 GOSUB 5000
1125 IF X1>3.75 THEN 1200
1150 GO SUB 3800
1175 GO TO 1225
1200 GOSUB 4100
1225 IF X1>2 THEN 1300
1250 GOSUB 5450
1275 GO TO 1550
1300 GOSUB 5850
1550 T1=2*M1*I3/(L1*A**2*3.14159)*L**2
1600 Z=((1-1)/(M-1))*L
1650 T2=(T1/(N#3.14159*((M1*L)**2+(N#3.14159)**2)))
1651 T2=T2*(1-X1*(K1+K2*I1/I2))*SIN(X1*Z/A)
1700 D=(N+1)/2-INT((N+1)/2)
1725 IF D <> 0 THEN 1740
1735 T2=T2*(1+EXP(-M1*L))
1735 GO TO 1750
1740 T2 =T2*(1-EXP(-M1*L))
1750 S=S+T2
1800 IF N4=4 THEN 2050
1850 S4=S4+ABS(T2)
1900 N4=N4+1
1950 N=N+1
2000 GO TO 850
2050 N4=0
2100 IF S4<=A1 THEN 2300
2150 S4=0
2200 N=N+1
2250 GO TO 850
2300 N=1
2325 S4=0
2350 T(I)=S-273.15
2352 T(I)=INT(T(I))
2375 PRINT "T("I") ="T(I)
2380 T(I)=S

```

```

2400      NEXT I
2401      PRINT
2404      PRINT
2406      PRINT
2414      PRINT
2416      PRINT
2418      PRINT "DO YOU WANT TO CALCULATE MORE TEMPERATURES?"
2420      INPUT B$
2430      PRINT
2435      PRINT
2440      IF LEFT(B$,1)="Y" THEN 99
2800      STOP
2830      REM*****SUBROUTINE S*****
2875      REM      FOR THE CALCULATION OF THE MODIFIED BESSEL FUNCTIONS
2876      REM      I0,I1,K0, AND K1 WORKING ON THE APPROPRIATE VOLUME VALUES
2901      REM SUBROUTINE IZER01
3000      T=X2/3.75
3050      I2=1+3.51562*T*T+3.08994*T**4+1.20675*T**6
3100      I2=I2+0.265972*T**8+0.0360768*T**10+0.0045813*T**12
3150      RETURN
3175      REM SUBROUTINE IZER02
3350      T=X2/3.75
3400      I2=0.39894228+0.01328592/T+0.00225319*T**(-2)
3450      I2=I2-0.00157565*T**(-3)
3455      I2=I2+0.00916281*T**(-4)-0.02057706*T**(-5)
3500      I2=I2+0.02635537*T**(-6)-0.01647633*T**(-7)
3550      I2=I2+0.00392377*T**(-8)
3551      I2=I2/((X2**0.5)*(EXP(-X2)))
3600      RETURN
3700      REM SUBROUTINE IONE1
3800      T=X1/3.75
3825      I1=0.5+0.87890594*T*T+0.51498869*T**4+0.1508493*T**6
3850      I1=I1+0.02658733*T**8+0.00301532*T**10+0.0032411*T**12
3851      I1=I1*X1
3900      RETURN
4000      REM SUBROUTINE IONE2
4100      T=X1/3.75
4150      I1=0.39894228-0.03988024/T-0.0036201*T**(-2)
4155      I1=I1+0.00163801*T**(-3)
4200      I1=I1-0.01031555*T**(-4)+0.02282967*T**(-5)
4250      I1=I1-0.02895312*T**(-6)+0.01787654*T**(-7)
4251      I1=I1-0.00420059*T**(-8)
4300      I1=I1/((X1**0.5)*EXP(-X1))
4350      RETURN
4450      REM SUBROUTINE KZER01
4600      X3=X2/2
4625      GOSUB 3000
4650      K2=-LOG(X3)*I2-0.57721566+0.42278420*X3**2+0.23069756*X3**4
4700      K2=K2+0.0348859*X3**6+0.00262698*X3**8+0.0001075*X3**10
4750      K2=K2+0.0000074*X3**12
4800      RETURN
4900      REM SUBROUTINE KZER02
5000      X3=2/X2
5050      K2=1.25331414-0.07832358*X3+0.02189568*X3**2-0.01062446*X3**3
5100      K2=K2+0.00587872*X3**4-0.0025154*X3**5+0.00053208*X3**6
5150      K2=K2/((X2**0.5)*EXP(X2))
5200      RETURN
5300      REM SUBROUTINE KONE1
5450      X3=X1/2
5475      GOSUB 3800
5500      K1=X1*LOG(X3)*I1+1+0.1544*X3**2-0.67278597*X3**4
5550      K1=K1-0.18156897*X3**6-0.01919402*X3**8-0.00110404*X3**10
5600      K1=K1-0.00004686*X3**12
5601      K1=K1/X1
5650      RETURN

```

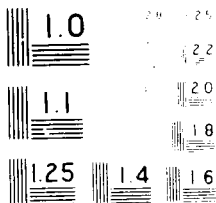
```
5700 REM SUBROUTINE KONE2
5850 X3=2/X1
5900 K1=1.25331414+0.23498619*X3-0.0365562*X3**2+0.0151427*X3**3
5950 K1=K1-0.00780353*X3**4+ 0.00325614*X3**5-0.00068245*X3**6
6000 K1=K1/((X1**0.5)*EXP(X1))
6050 RETURN
8000 END
#
```

References

1. Lockhart, L. B. Optics and Laser Technology 6(4), 159-65 (1974)
2. Karlov, N. V. Applied Optics 13(2), 301-9 (1974)
3. Oraevsky, A. N. Trends in Physics: Vol. of Plenary Lectures at the 2nd Gen. Conference, Euro. Phys. Soc. 95-124 (1973)
4. Zare, R. Scientific American p. 89 (Feb. 1977)
5. Glatt, I. and Yogev, A. J. Am. Chem. Soc. 98(22) 7087-8 (1976)
6. Adamson, A. W. A Textbook of Physical Chemistry Academic Press (1973), p. 153, 638
7. Basov, N. G.; Oraevsky, A. N.; and Pankratov, A. V. Biological and Chemical Applications of Lasers Academic Press (1974) pp. 203-229
8. Freeman, M. P. and Travis, D. N. J. Chem. Phys. 60(1) 231-6 (1974)
9. Kim, P. H.; Namba, S.; and Taki, K. Bulletin of the Chem. Soc. of Japan 47(2) 493-4 (1974)
10. Quel, E. and DeHemptinne, X. Annales de la Société Scientifique de Bruxelles 83(2) 262-76 (1969)
11. Richardson, M. C. and Isenor, N. R. Optics Communications 5(5) 394-7 (1972)
12. Karny, Z.; Ronn, A.; Weitz, E.; and Flynn, G. Chem. Phys. Letters 17(3) 347-50 (1972)
13. Grabiner, F. r. and Flynn, G. W. J. Chem. Phys. 60(2) 398-401 (1974)
14. Berry, M. J. J. Chem. Phys. 61(8) 3114-43 (1974)
15. Lyman, J. L. and Rockwood, S. D. J. Applied Phys. 47(2) 595-601 (1976)
16. Thomas, J. K. Advan. Radiat. Res., Phys. Chem. 1 303-9 (1973)

17. Letokhov, V. S. Physics Today 23-31 (May 1977)
18. Ambartzumian, R. V. and Letokhov, V. S. Accounts of Chem. Research 10, p.61 (1977)
19. Oraevsky, A. M. and Pankratov, A. V. Lect. Notes Phys. 43, 304-23 (1975)
20. Earl, B. L. and Ronn, A. M. Chem. Phys. Letters 41(1) 29-32 (1976)
21. Riley, C.; Shatas, R.; and Opp, L. "Low Power CO₂ Laser Induced Chemistry of SF₆ Sensitized Diborane", Inorganic Chem. (Not yet published)
22. Herrick, R. S. Undergraduate Thesis: CO₂ Laser Induced Decomposition of Freon 113, Union College Chemistry Department, 1978
23. Larsen, D. M. and Bloembergen, N. Optics Communications 17(3) 254-8 (1976)
24. Brown, C. Undergraduate Thesis, Union College Chemistry Department, 1977
25. Mann, D.; Acquista, N.; and Plyer, E. J. Chem. Phys. 21 p. 1949 (1953)
26. Bernstein, R.; Zietlow, J.; and Cleveland, F. J. Chem. Phys. 21 p. 1778 (1953)
27. Silverstein, R.; Bassler, G.; and Morrill, T. Spectro-metric Identification of Organic Compounds (3rd Ed.) John Wiley and Sons, Inc. (1974) p. 85
28. Zitter, R. and Koster, D. J. Am. Chem. Soc. 98(6) 1613-14 (1976)
29. Ronn, A. M. Spectroscopy Letters 8(5) 303-28 (1975)
30. Bailey, Cruickshank, Farrell, Horne, North, Wilmont, and Win J. Chem. Phys. 60(5) 1699-1704 (1974)
31. Knudtson, J. and Eyring, E. U.S. National Technical Information Service AD 777 460/776A (1974)
32. Yogev, E.; Loewenstein, R.; and Amar, D. J. Am Chem. Soc. 94 1091-6 (1972)
33. Klein, F.; Lussier, F.; and Steinfeld, J. Spectroscopy Letters 8(5) 247-61 (1975)
34. Lowry, T. and Richardson, K. Mechanism and Theory in Organic Chemistry Harper and Row (1976) p. 473

END



Photographed with a Zeiss Ikon camera